



Norwegian University of
Science and Technology

Numerical Modelling of Arctic Coastal Hydrodynamics and Sediment Transport

Benedicte T Borgersen

Civil and Environmental Engineering

Submission date: June 2016

Supervisor: Raed Khalil Lubbad, BAT

Co-supervisor: Øivind A. Arntsen, BAT

Norwegian University of Science and Technology
Department of Civil and Transport Engineering

Acknowledgement

I would like to express my sincere gratitude to my supervisor, Dr. Raed Lubbad for his guidance, help, understanding and encouragement during this semester and the previous when I wrote my project thesis. I am thankful to all my professors at Norwegian University of Science and Technology. I also want to acknowledge Danish Hydraulic Institute(DHI) for license files, help and support concerning my master thesis. I am grateful to Emilie Guegan, post doc at Norwegian University of Science and Technology for comments and discussions. I want to acknowledge Mohammad Saud Afzal, Phd candidate at Norwegian University of Science and Technology for his help in learning MIKE21 used in this thesis

Abstract

Coastal areas are experiencing an increase in human population and activities, both in temperate and in Arctic areas. This change in the coastal areas requires that the areas are safe and reliable in order to not put human lives and economical values in danger. To be about to protect the coastal areas it is important to know the hydrodynamics and sediment transport and their effect on coastal areas.

Numerical modeling of coastal hydrodynamics and sediment transport is a normal approach to evaluate coastal engineering problems. Many numerical modeling tools are developed for temperate areas but there are not so many programs developed to investigate the Arctic coastal erosion. This thesis written at Norwegian University of Science and Technology(NTNU) is researching Bjørndalen at Svalbard and the coastal erosion that took place because of the storm in 2015.

This study investigates the possibility to model the hydrodynamics in an Arctic area and further to be able to use an numerical modeling tool to investigate the Arctic coastal erosion. The numerical tool used in this thesis is MIKE21 developed by Danish Hydraulic Institute(DHI). MIKE21 is a coastal modelling program developed to be used in coastal and marine environments.

The results of modelling the coastal hydrodynamics in Isfjorden where Bjørndalen is located is not perfect and they have some unrealistically errors in the results. Bjørndalen is located at a site where the lack of measured data makes it difficult to calibrate the model. In this case the model was not calibrated as it should have been. This study will be a beginning to be able to predict the evolution of out coastal zones in the Arctic. Hopefully it will be found ways to predict coastal erosion in the Arctic, witch in turn will make it possible to protect the coast from damage.

Sammendrag

Befolkningsvekst og økt industriell aktivitet i kystområdene verden over er et kjent fenomen, store deler av verdens befolkning er nå bosatt i områder med nær tilknytning til kystområder. Denne økningen krever at områdene er sikre og pålitlige i mange år fremover for å ikke risikere tap av menneskeliv og økonomisk verdi. Numerisk modellering er en vanlig fremgangsmåte når man undersøker hydrodynamisk oppførsel og sediment transport i kystområder. Mange numeriske modeller er utviklet til å modellere og undersøke kystområder i tempererte områder, programmer til å modellere de Arktiske forholdene er det ikke like mange av. Denne Master oppgaven som er skrevet på Norges Teknisk Naturvitenskapelige Universitet(NTNU) er en studie som skal undersøke den hydrodynamiske oppførselen under stormen på Bjørndalens kystline på Svalbard i 2015. Denne stormen førte til store eroderte områder langs kysten hvor hytter og veier ble liggende i utsatte posisjoner.

Denne studien undersøker mulighetene for å kunne modellere den hydrodynamiske oppførselen i et Arktisk område for å videre kunne ha muligheten til å forutsi erosjon som skjer på grunn av den hydrodynamiske oppførselen i området. MIKE21 utviklet av Danish Hydraulic Institute(DHI) og det numeriske programmet som er i bruk i denne studien. MIKE21 er utviklet til bruk i kyst og marine områder.

Resultatet fra studiens modellering av de hydrodynamiske prosessene i Isfjorden er ikke helt optimale. Det er noen urealistiske høye verdier på strømminger i noen områder i Isfjorden, samt generelt litt for lave bølgehøyder når de modelerte døunningen som kommer inn i Isfjorden er grunnlaget. Døunningene er modellert av NMI(Norges Meteorologiske Institutt). Bjørndalen er lokalisert på Svalbard hvor det ikke finnes målestasjoner for bølger eller havnivå, dette gjorde det vanskelig å kalibrere modellen, noe som burde vært gjort. Denne studien er gjennomført for å kunne ha muligheten til å forutsi kystens evolusjon når den er påvirket av et endret klima og de på følgende endringene dette har på de Arktiske områdene.

Preface

This thesis studies coastal hydrodynamics and sediment transport in the Arctic. The objective of the thesis has been to validate numerical tools such as MIKE21 by DHI for estimating coastal hydrodynamics and sediment transport in the Arctic. In September 2015 Bjørndalen at Svalbard experienced large erosion in its coastal zone. This site has been chosen for this project as a case study. A numerical modulation of the storm in 2015 has been carried out.

Table of Contents

Acknowledgement	1
Abstract	i
Sammendrag	ii
Preface	iii
Table of Contents	vii
List of Tables	ix
List of Figures	xii
1 Introduction	1
1.1 Background And Motivation	1
1.2 Structure Of The Thesis	2
2 Coastal Hydrodynamics and Sediment Transport	3
2.1 Introduction	5
2.2 Coastal Hydrodynamics	6
2.2.1 Waves	6
2.3 Wave Transformation	12
2.3.1 Current	16
2.4 Sediment Transport	18
2.4.1 Sediment Properties	19
2.4.2 Bed load Transport	19
2.4.3 Suspended Load Transport	21
2.4.4 Soulsby-Van Rijn Formula	22
2.5 Morphological Processes	24
2.6 Modeling For Coastal Hydrodynamics and Sediment Transport	24

3	Arctic coastal erosion	25
3.1	Introduction	27
3.2	Thermal Erosion Processes	27
3.2.1	Thermo Denudation	28
3.2.2	Thermo Abrasion	29
4	Numerical Modeling	31
4.1	Introduction	31
4.2	MIKE21	32
4.2.1	MIKE21 Flow Hydrodynamic (HD)	32
4.2.2	MIKE21 Spectral Waves (SW)	33
4.2.3	MIKE21 Sediment Transport (ST)	33
5	Case study	35
5.1	Introduction	35
5.2	Description of Area	37
5.2.1	Bathymetry	37
5.2.2	Wind	39
5.2.3	Waves	43
5.2.4	Water level	45
5.2.5	Sediment properties	47
5.3	Numerical model setup	47
5.3.1	Model Setup for MIKE21 Flow HD	47
5.3.2	Model Setup for MIKE21 Spectral Wave	49
5.3.3	Sediment transport	50
6	Results and discussion	51
6.1	MIKE21 Flow HD	51
6.1.1	Run#1, Constant wind data from NMI and tides from C-map	52
6.1.2	Run# 2: Varying wind data from ECMWF and tides from C-map	54
6.1.3	Run#3, Constant Wind Data From NMI, No Tides	55
6.1.4	Run#4: Varying Wind Data From ECMWF, No Tides	56
6.1.5	Discussion	57
6.2	MIKE21 Spectral Wave Module Result	59
6.2.1	Run#1: Offshore Waves From NMI , Varying Wind From ECMWF, Water Elevation and Currents From MIKE21 Flow HD	59
6.2.2	Run#2: Varying Wind from ECMWF, Water Elevation and Currents From MIKE21 Flow HD	64
6.2.3	Run#3: Offshore Waves From NMI, Water Elevation and Currents From MIKE21 Flow HD	67
6.3	Discussion	70
6.3.1	Discussion	71
6.4	Sediment Transport	72

7 Conclusion and Recommendation	73
7.1 Summary	73
7.2 Recommendation For Further Work	74
Bibliography	75

List of Tables

5.1	Middle Wind speed at Svalbard airport correlated for measurement height using power law	42
5.2	Middle Wind speed at Svalbard airport without correlation for measured height	42

List of Figures

2.1	Simple representation of a basic wave(Rafael E. Vasquez1 and Correa (2014))	7
2.2	Example of surface elevation time series	9
2.3	Example on how an energy spectrum can look like(Krogstad and Arntsen (2003))	10
2.4	Water particle motion in shallow water and deep water. Based on figure(Krogstad and Arntsen (2003))	13
2.5	Illustration of waves shoaling	14
2.6	Illustration of waves refraction(Carleton,2016)	15
2.7	Shields Diagram(MIT, 2015)	20
3.1	Thermo Denudation process(Gugan and Christiansen (2016a))	28
3.2	Description of thermal abrasion process(BBC (2016))	29
5.1	Area map showing the location of Bjørndalen at Isfjorden on Svalbard	36
5.2	Isfjorden bathymetry for MIKE C-MAP	38
5.3	Wind speed for Isfjorden Radio, black is NMI and blue is ECMWF	40
5.4	Wind speed for Barentsburg, black is NMI and blue is ECMWF	40
5.5	Wind speed for Svalbard Airport, black is NMI and blue is ECMWF	40
5.6	Wind direction for Isfjorden radiostation	41
5.7	Wind direction for Svalbard airport	41
5.8	Wind direction for Barentsburg	42
5.9	Wave height for the wave conditions modeled by NMI	44
5.10	Swell wave height over direction for 27 September to 4 October	44
5.11	Water elevation at Bjørndalen	45
5.12	Water elevation at Hammerfest in Finnmark, Norway	46
6.1	Mesh over Bjørndalen with the location the data is extracted from	51
6.2	Water elevation at Bjørndalen with wind data from NMI, run number one	52
6.3	Current at Bjørndalen with wind data from NMI	53

6.4	Current speed and direction at Bjørndalen caused by wind data from ECMWF and tidal variation	53
6.5	Water elevation at Bjørndalen with wind from ECMWF, run number two	54
6.6	Current velocity and current direction at Isfjorden using data from ECMWF	54
6.7	Water elevation at Bjørndalen with wind input from NMI and tides are neglected	55
6.8	Currents in Isfjorden with wind input from NMI and tides are neglected	55
6.9	Water elevation at Bjørndalen with wind input from ECMWF and tides are neglected	56
6.10	Current speed in Isfjorden with wind input from ECMWF and tides are neglected	56
6.11	Significant (H_s) and maximum wave height (H_{max}) at Bjørndalen	59
6.12	Wind velocity at Bjørndalen	60
6.13	Maximum wave height at Bjørndalen	60
6.14	Significant wave height at Bjørndalen	61
6.15	Wave period at Bjørndalen	61
6.16	Wave direction at Bjørndalen	62
6.17	Radiation stresses at Bjørndalen	63
6.18	Wave height at Bjørndalen when swell are neglected	64
6.19	Wave period at Bjørndalen, when swell are neglected	65
6.20	Radiation stress at Bjørndalen when swell are neglected	65
6.21	Current at Bjørndalen when swell are neglected	66
6.22	Wave height at Bjørndalen when wind is neglected	67
6.23	Current velocity at Bjørndalen when wind is neglected	68
6.24	Radiation stresses at Bjørndalen when wind is neglected	68
6.25	Wave period at Bjørndalen when wind is neglected	69
6.26	Current at Bjørndalen	71

Introduction

1.1 Background And Motivation

The coast is a complicated dynamic system between the marine environment and terrain above water. The coastal zone is constantly changing, eroding some places and accretion other places. Coastlines around the world are different and have many varying properties. Sandy beaches, rocky shorelines, islands, bays, glaciated coasts are just some of the many different types of coastlines that can be found. All the different coastlines make different physical properties. The dynamics of the coastlines are always different, but they all have some similarities. For example a sandy beach will have erosion where the sand is moved away from the beach to a offshore location during the winter and accretion where the sand is moved up on the beach during the summer. Sea cliffs will behave differently, they may be eroded during a storm or if the cliff loses its stability and it will never go back to its original profile(Sorensen (1997)).

Through out history coastal evolution has been an important issue. Coastal areas have always been an important area for human activities and they continue to be important. In coastal areas, industries and number of real estate properties are increasing. Hence more economical value and human lives depend on safe infrastructure in case of a natural hazard. Large amount of the worlds population live and work in coastal areas and these numbers are increasing(Ashbindu Singh (2006)).

The World is experiencing a global climate change. Some of the changes are manifested as increase in temperature, increase in storm frequency and intensity and finally as an increase in water level (NASA (2016b)). Because of the climate change and the increase in human population and activities in coastal areas, it becomes more important than ever to protect these areas. To be able to protect these areas it is important to be able to predict a potential storm and the consequences of the storm. Coastal erosion is caused by coastal actions and can cause large economical damage by damaging constructions and remove ground material.

The Arctic area is also experiencing the climate change, maybe more than temperate areas. Here the most important factor is the increasing temperature. Traditionally, the Arctic water is covered by sea ice for long period each year. This protects the coastline in the Arctic from environmental action coming from waves. Due to the increase of temperatures, the ice free periods in the Arctic are getting longer and the coastal zone is more exposed to the environmental forces. Similar to the conditions elsewhere the storm intensity and frequency are also increasing in the Arctic.

Bjørndalen is a site located at Svalbard. This site was hit by a storm that led to considerable damage to cabins and roads nearby(Barstein (2015)).

The behavior of the ocean, waves, tides and wind are complex systems that are difficult to investigate. Numerical models are therefore a good tools to investigate coastal areas. But the models are developed for non-Arctic environments and the use of good numerical modelling of areas that are characterised as Arctic environments need to be done.

1.2 Structure Of The Thesis

The thesis consists of seven chapters. The first chapter is an introduction and states what the thesis is about. Chapter number two discusses the properties of Arctic coastal erosion and mechanisms. The third chapter discusses the properties of Arctic coastal erosion mechanisms. Chapter number four introduces the different modules of MIKE21 which is a computer program developed by Danish Academy of Technical Science (DHI) for simulation of coastal hydrodynamics and sediment transport. The 2015 storm in Bjørndalen is used as a case study. Chapter number five describes the Bjørndalen site and explains the setup of the numerical model. Chapter six presents the results from the numerical model and the final chapter seven gives a conclusion and recommendations for future work.

Chapter **2**

Coastal Hydrodynamics and Sediment Transport

2.1 Introduction

Definition of coastal morphodynamics is the interaction between hydrodynamics and the seabed. The coastline is always subjected to changing physical environmental forces. These forces are for example wind, waves, tides, currents, rain, ice etc. Coastal morphodynamics are about how the hydrodynamic forces and the coastal seabed is acting together. Physical processes will always be present and the hydrodynamics can change the seabed and a changed seabed can change the hydrodynamics. Morphodynamics are temporal and spatial scaled system, where the time range can be hours, days, months and year and the scale can vary from one harbor to a long coastline. The time and scale depends on the engineering project. When it comes to coastal engineering, every location has its own characteristics. Included in an analysis the natural conditions, human activities and the sediments need to be investigated, but the most important thing to investigate is the interaction between them.

The energy from moving water in waves and current can cause sediment transport in coastal areas. There are mainly two different types of sediment transport called long shore and cross shore sediment transport. These two types of sediment transport are very different and are caused by different physical phenomena, but they can occur at the same time.

Sediment transport, coastal erosion and accretion is created by moving water in form of current and waves. The properties of the sediments grain size, porosity and density are important factors when investigating the sediment transport.

2.2 Coastal Hydrodynamics

Coastal hydrodynamic is the physical behavior of movements in coastal areas, this includes waves, currents, tides and wind and the behavior of them in a coastal location. Wind waves are created by wind, and the physical properties of the waves are; wave height(H), wave period(T), wave length(λ). The properties of the waves depend on the speed, duration and fetch(Kamphuis (2010)). Energy of the wind is transformed to energy in form of waves. The wave energy can then again be transformed into currents, move sediment particles or other forms of energy.

Waves can be generated in offshore areas and move in different directions. When the waves are in an offshore location they are usually weakly non-linear and can be assumed to have linear behavior and linear wave theory applies(Krogstad and Arntsen (2003)). When the waves are propagating into shallow or intermediate water they will be affected by the water depth and non-linear processes start.

The phenomena the waves are experiencing when non-linear processes start to work are called wave transformation. Some important wave transformations are wave breaking, shoaling, refraction, diffraction etc. The sediment transport is a result of these phenomena because the energy dissipated by these phenomena are creating currents both cross shore and long shore currents.

2.2.1 Waves

Waves are one of the natural forces acting on coastal areas. Waves are changing water elevating over time and space(Krogstad and Arntsen (2003)). The simplest way of describing waves is by linear wave theory. Linear wave theory is a simplification and the waves are simplified by using sinusoidal representation (Krogstad and Arntsen (2003)). Waves are simply described with wave period T , wave length λ and wave height H . The wave profile is given in equation 2.1. η is the water elevation from SWL (sea water level), k is the wave number and ω is the angular wave frequency(Kamphuis (2010)). The profile of a wave is shown in figure 5.1. According to this theory water particles are moving in orbital motions and this physical behavior is the main assumption behind wave transformation.

There are different types of waves some of them wind waves, tidal waves tsunamis, seiche, ect. These waves are created by different physical phenomena. The most common type is wind waves and are the type of wind produced during a storm. These types of waves are generated by wind blowing over an area. The characteristics of the waves then depend on the fetch, wind speed and duration of the wind blowing(Kamphuis (2010)).

$$\eta = \eta(x, t) = \frac{H}{2} \cos(kx - \omega t) \quad (2.1)$$

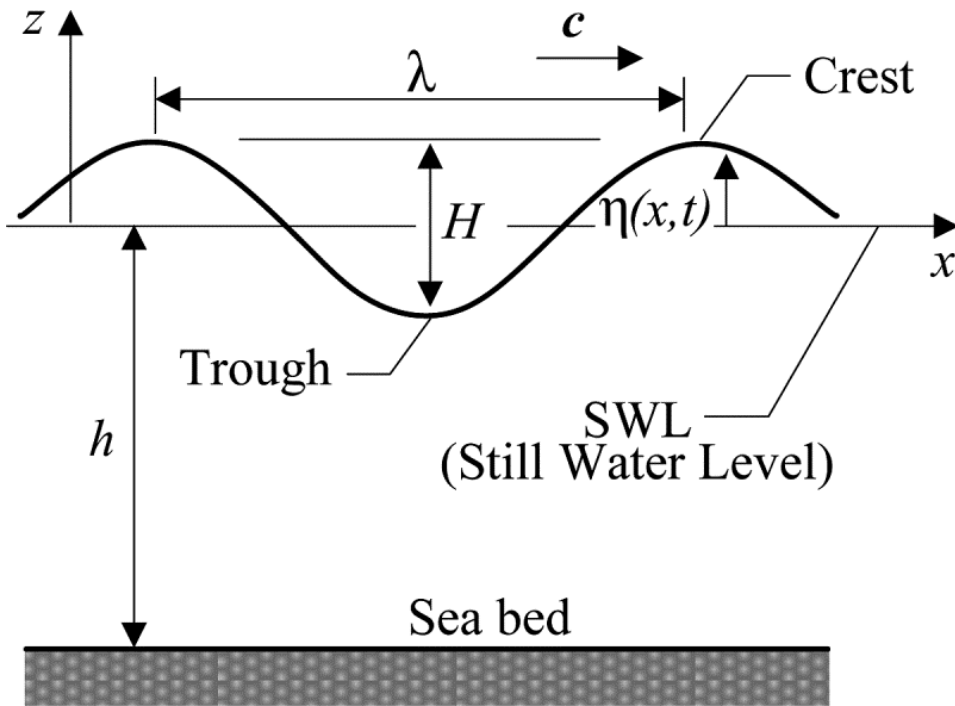


Figure 2.1: Simple representation of a basic wave (Rafael E. Vasquez1 and Correa (2014))

Wind Generated Waves

Wind generated waves, also called surface gravity waves are generated by the sum of momentum between water surface and wind (Bretschneider (1952)). This momentum from the stresses on the water surface from the wind (Roelvink and Reniers (2012)). The shape and size of the waves depend on magnitude of the wind, the fetch and the duration of the storm (Kamphuis (2010)). The wind are transforming energy over to waves, so when the wind stops blowing the waves will travel until they interact with an obstacle or reach shallower water and eventually the coastline.

Waves in deep water are usually irregular and exist of a variety of wave heights, wave lengths and wave periods. The sea state will therefore be described as a number of independent waves added together (Krogstad and Arntsen (2003)). The sea state is usually described as a Gaussian distribution consisting of irregular waves. These waves can be calculated with linear wave theory, but as the waves propagate into shallow water they will feel the bottom and non-linear wave theory are needed (Roelvink and Reniers (2012)).

There are two types of wind waves that are important when investigating sediment transport caused by a storm. These two types of wind are called swell and sea.

Sea

Sea is locally generated and are highly irregular waves with different wave height and wave length. Generally these waves have short wave lengths and is easily affected by wind. These waves are often found in areas close to the shoreline, in fjords or similar where the travelling distance is short. This is the reason for the small wave heights and short periods, they have not enough space to develop to waves with long period and more regular waves.(Roelvink and Reniers (2012))

Swell

Swell is defined as waves that have left their place of origin, they usually have long wavelength and are highly regular. Swell can travel thousands of km before they reach shore, and these waves can hit the shore even if there is no wind. Because of the long travelling distance the waves are developing from irregular sea to regular sea. Swell have a more constant wave height and wave period, they are usually travelling in groups of waves and these waves have high energy when they reach shore and may have a higher wave height due to the conditions at the place of origin. (Roelvink and Reniers (2012))

Spectral Description

A normal way to represent the wave climate is by using spectral description instead of deterministic representation of wave data. Spectral description is a statistically representation of the sea state in an location using statistical parameters. When looking at irregular sea it is decomposed into many sinusoidal waves with different wave heights and wave periods(Krogstad and Arntsen (2003)). When these waves are added together using superposition the result will be irregular wave conditions. The new equation for surface elevation when sinus waves are added together is shown in (2.2), with a_n being the amplitude of each individual wave, k_n and ω_n are wave parameters depending on period and wavelength respectively. This description of the surface elevation does not consider the directional spread of waves, if this have to be included additional methods need to be applied(Krogstad and Arntsen (2003)).

The sea state can be represented by spectral representation and with Fourier analysis the wave height and wave period can be found. This can also be represented with an energy spectrum witch is given in equation 2.3. This switch between surface elevation and spectral description is shown in figure 2.3 and 2.2.

This type of describing the sea state is more practical due to the fact that it is very hard to take out important information when only looking at the surface elevation. In addition one of the important factors about the sea state is the energy produced and the effect the energy will have when interacting with shoreline and structures and not so much the properties of the different waves during a period of time.

$$\eta(x, t) = \sum_{i=1}^N a_n \cos(\omega_n t - k_n x - \phi_n) \quad (2.2)$$

To find the wave spectrum the wave energy E is important and shown in (2.3). here ρ is the density of water, g is the gravity, η is the surface elevation and Ψ represents the density of waves corresponding to different $k=2\pi$. The equation is from the (Krogstad and Arntsen (2003)).

$$E = \rho g \text{Var}(\eta) = \int_k \Psi(k) d^2 k \quad (2.3)$$

Equation (2.3) gives the energy spectrum, the amount of energy depends on the frequency. The frequency is dependent on the wave length and wave height. Long and high waves give lower frequency, while short and small waves amplitude waves give higher frequency concentration in the spectrum.

In figure 2.3 and figure 2.2 the corresponding wave spectrum and surface elevation is shown as an example.

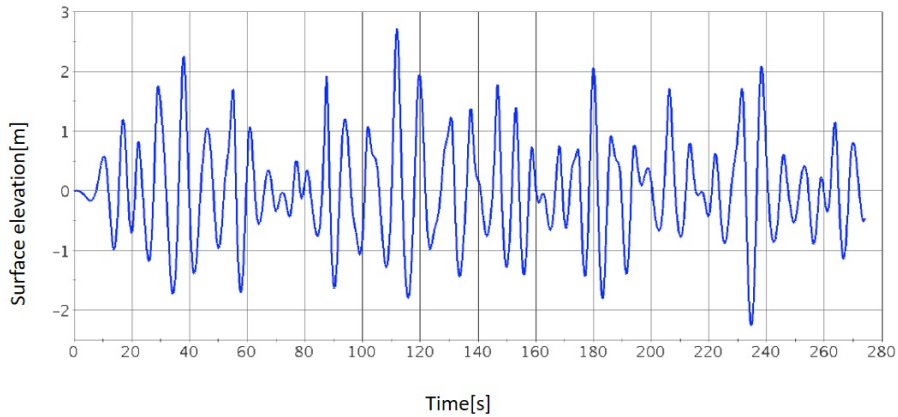


Figure 2.2: Example of surface elevation time series

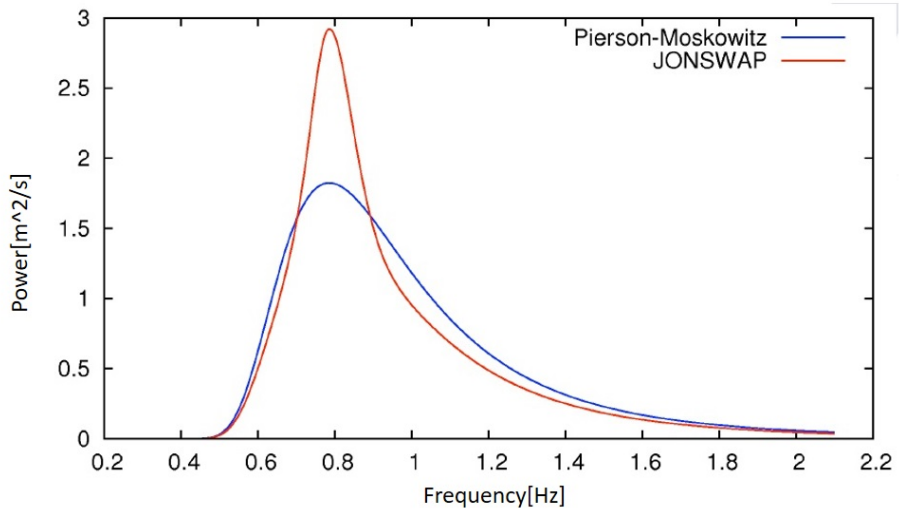


Figure 2.3: Example on how an energy spectrum can look like(Krogstad and Arntsen (2003))

Wave Energy

The wave energy is one of the main forces that have an impact on the coastal environments. All processes occurring in coastal areas are arise from the wave energy and the total energy of the waves impact on the shoreline. Conservation of energy is the assumption behind the wave transformation when waves propagating from deep water conditions to shallow water(Roelvink and Reniers (2012)). Equation 2.4(Kamphuis (2010)) and equation 2.6(Roelvink and Reniers (2012)) show the energy conservation equation and arising from waves respectively. The wave Energy spectrum can be used to describe variations in time and space, the simplest form is when the wave spectrum is integrated over all frequencies. This energy balance is shown in equation 2.5(Roelvink and Reniers (2012)).

$$\Delta \cdot (EC_g) = 0 \quad (2.4)$$

$$\frac{\partial E_w}{\partial t} + \frac{\partial}{\partial x}(E_w c_w \cos(\theta_m)) + \frac{\partial}{\partial y}(E_w c_g \sin(\theta_m)) = -D_w - D_f \quad (2.5)$$

In equation 2.5 E_w is the wave energy and depends on H_{rms} shown in Equation 2.6. c_g is the energy velocity, θ_m is the mean wave direction, D_w is the wave energy dissipation due to breaking waves and D_f is the bottom friction and E_w is the energy shown in equation 2.6 where ρ is the water density, g is the gravity and H_{rms} is the root-mean-square wave height.

$$E_w = \frac{1}{8} \rho g H_{rms}^2 \quad (2.6)$$

Roller Energy

Waves start to break in the beginning of the transitional zone and at the point of breaking the wave energy will produce surface rollers. Surface rollers is in the transitional zone there will be a temporarily storage of shoreward momentum(Roelvink and Reniers (2012)). The transitional zone ends where the wave setup starts and cross shore currents can be found due to the breaking waves. The roller energy can be found by equation 2.7(Roelvink and Reniers (2012)). In this equation E_r is the Roller energy, D_w is the loss of organized wave motion due to breaking waves, D_r is the roller energy dissipation and θ_m is the mean wave direction. The roller energy is working to swirl up lose sediments.

$$\frac{dE_r}{dt} = \frac{\partial E_r}{\partial t} + \frac{\partial E_r \cos \theta_m}{\partial x} + \frac{\partial E_r \sin \theta_m}{\partial y} = D_w - D_r \quad (2.7)$$

2.3 Wave Transformation

Waves that are generated at an offshore location are weakly non linear and can be described using linear wave theory as they are weakly non-linear. When waves are affected by non-linear properties other theories need to be used and the properties of the waves change, and this is called wave transformation. Waves that travel from an offshore location will reach shallower water and it is between deep water and shallow water the transformation begins.

The transformations the waves are experiencing are wave breaking, shoaling, refraction, diffraction etc. Wave transformation equations describe the change in wave behavior due to the conservation of energy in waves(Kamphuis (2010)). The conservation of energy goes into changing the direction of the waves found by wave propagation equation shown in equation 2.8.

In figure 2.4 the orbital motion of water particles are shown(Krogstad and Arntsen (2003)). The motion for shallow and transitional water depth are shown at left and for deep water at right. When the water depth is decreasing the motions of the water particles starts to interact with the sea bottom and the waves will start to transform. When the water particles interact with the bottom the non linear physics will start to apply.

The transformation of waves depend on the conservation of energy flux equation and wave propagation equation(Kamphuis (2010)).

$$\nabla \times \mathbf{k} = 0 \quad (2.8)$$

$$\nabla \cdot (E\mathbf{C}_g) = 0 \quad (2.9)$$

In equation 2.8 \mathbf{k} is the wave number vector and gives the directions of the waves. In 2.9 E is the energy flux and $\mathbf{C}_g = n\mathbf{C}$ is the group velocity vector and is a wave parameter depending on water depth and the wave number \mathbf{k} . n is the group velocity parameter and \mathbf{C} is velocity of propagation. With equation 2.8 and 2.9 different wave transformations can be derived.

$$E = \frac{1}{8} \rho g H^2 \quad (2.10)$$

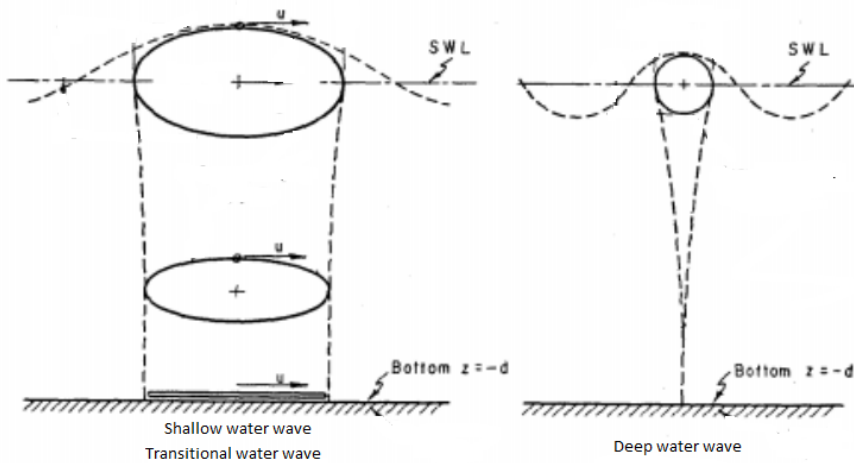


Figure 2.4: Water particle motion in shallow water and deep water. Based on figure(Krogstad and Arntsen (2003))

Shoaling

Shoaling is when the wave height increases in decreasing water depth(RRoelvink and Re-niers (2012)). The shoaling equation 2.11 describes the relationship between wave height and water depth, the equation is derived from the conservation of energy equation 2.10. The bathymetry of the coastal area is important for how the shoaling process is happening, when the water depth is decreasing the wave height is increasing until the waves break. The waves will break when they reach their limited steepness(Kamphuis (2010)). This can be seen in figure 2.5. $EC_g = constant$ and equation 2.11 gives the relationship between the wave height at two different water depths, that is developed from the energy conservation formula.

$$\frac{H_2}{H_1} = \sqrt{\frac{n_1 C_1}{n_2 C_2}} \quad (2.11)$$

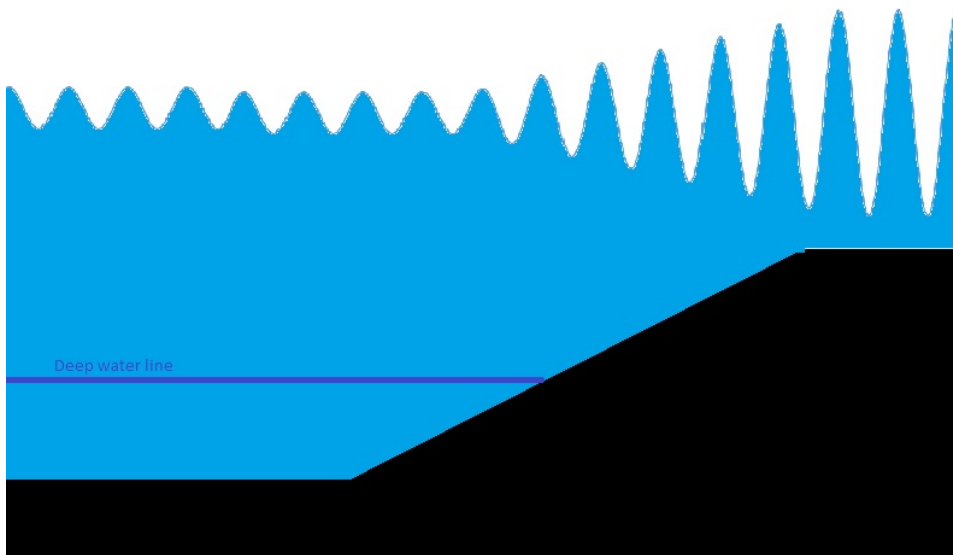


Figure 2.5: Illustration of waves shoaling

Refraction

Refraction is the change in wave direction when waves approach shore (Kamphuis (2010)). If waves approach the shoreline at an angle, refraction will happen at the same time as Shoaling. The waves will interact with the bottom so the wave crest will change direction and meet the shore at a straighter line. What happens is that when waves going into a shallow area their velocity will decrease because energy will be lost in interaction with the seabed. The wave crest will be bent and the wave crest becomes parallel to the bottom contours. Refraction can also be determined by Equation 2.12 (Kamphuis (2010)). The equation is based on the conservation of energy. If the shoreline is not straight but have a curve, the refraction can happen in different direction and wave energy can be concentrated at hotspots along the shoreline, energy can be localized as shown in figure 2.6. The refraction of wave are also often described by Snell's law and the equation is given in equation 2.13 and 2.14(Kamphuis (2010))

$$\frac{H_2}{H_1} = \sqrt{\frac{n_1 C_1}{n_2 C_2}} \sqrt{\frac{b_1}{b_2}} \quad (2.12)$$

$$\frac{\sin\alpha_2}{\sin\alpha_1} = \frac{C_2}{C_1} \quad (2.13)$$

$$\frac{\sin\alpha}{\sin\alpha_0} = \frac{C}{C_0} \quad (2.14)$$

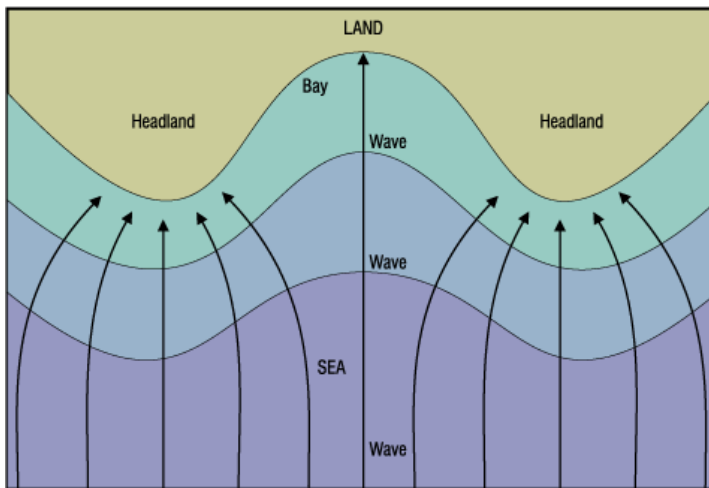


Figure 2.6: Illustration of waves refraction(Carleton,2016)

Breaking Waves

The wave height will increase due to the shoaling effect when waves propagated into shallow water. Eventually the waves will reach the limiting steepness and they will start to break (Kamphuis (2010)). The waves start to break and the energy in the waves transform to turbulence and movement in the water. The breaking waves have many different breaking forms surging, collapsing, plunging and spilling (Galvin (2016)). The concentrated energy from these waveforms are important and depend on the slope of the sea bottom. The breaking conditions are described in equation 2.15 (Kamphuis (2010)). In the equation H_b is the breaking wave height, L_b is the breaking wave length and d_b is the water depth for the corresponding wave height and wavelength.

$$\frac{H_b}{L_b} = 0.14 \tanh\left(\frac{2\pi d_b}{L_b}\right) \quad (2.15)$$

2.3.1 Current

Coastal currents play an important role in coastal morphology. Currents are the natural force that is transporting sediments in the coastal zones. There are different kinds of currents acting along the coast and they are generated by different natural processes. Wind induced currents, wave induced currents and tidal currents are some types of currents that can be found in coastal areas (Roelvink and Reniers (2012)).

Waves propagate towards the shore and if they approach the shore at an angle the waves will break with an angle to the shore. In the breaking zone there will be created a momentum along the shoreline that will cause a long shore current (?). This type of currents is called wave induced currents, Wind currents will be caused by the relationship between wind and water surface shear stress, undertow currents caused by water washed up on the beach retreating back to the ocean and there can also be currents because of nearby rivers. Tidal currents arise because of changing tides (Roelvink and Reniers (2012)).

Wave-driven currents arise from the radiation stresses caused by the waves. This current can be very strong in the surf zone where the waves break and gives a large attribute to sediment transport in the direction of the waves propagation (Fredsoe and Deigaard (1992)).

Storm Surge

A storm surge is increasing water elevation during a storm. The reasons for the increasing water level is difference in pressure, a low pressure over an area will make the water level rise. The other reason can be wind piling onshore and pushing the water onto the shoreline. Previous in this report it is mentioned the presence of a large storm surge during the storm of interest in September 2015. Storm surge is when the water level is high due to wind blowing the water onshore and difference in high and low pressure. (hurricane center (2016))

Radiation Stresses

Radiation stress is a flow of momentum that is caused by the presence of waves in a coastal area (LONGUET-HIGGINS and STEWART (1964)). Radiations stresses from waves are one of the factors that causes wave-setup, this gives and additional increase of water level at the shoreline.

Shallow water equations

Shallow water equations are important to understand currents in close shore areas, they are derived from Navier-Stokes equations and takes into account the momentum balance and Boussinesq (Roelvink and Reniers (2012)). The shallow water equations have included the processes from the sections before and they are either solved for two dimensional or three dimensional. The equations are partially differential equations that describes the behavior of water under the free surface with processes that are described earlier is included. The shallow water Equations are 2.3.1, 2.17 and 2.18.

$$(2.16) \quad \frac{\partial \rho u}{\partial t} + u \frac{\partial \rho u}{\partial x} + v \frac{\partial \rho u}{\partial y} + w \frac{\partial \rho u}{\partial z} - f_{cor} \rho v = \left(\frac{\partial \sigma_{xx}}{\partial x} + \frac{\partial \tau_{xy}}{\partial y} + \frac{\partial \tau_{xz}}{\partial z} - \frac{\partial p}{\partial x} \right)$$

$$\frac{\partial \rho v}{\partial t} + u \frac{\partial \rho v}{\partial x} + v \frac{\partial \rho v}{\partial y} + w \frac{\partial \rho v}{\partial z} - f_{cor} \rho u = \left(\frac{\partial \tau_{yx}}{\partial x} + \frac{\partial \sigma_{yy}}{\partial y} + \frac{\partial \tau_{yz}}{\partial z} - \frac{\partial p}{\partial y} \right) \quad (2.17)$$

$$\frac{\partial \rho w}{\partial t} + u \frac{\partial \rho w}{\partial x} + v \frac{\partial \rho w}{\partial y} + w \frac{\partial \rho w}{\partial z} = \left(\frac{\partial \tau_{zx}}{\partial x} + \frac{\partial \tau_{zy}}{\partial y} + \frac{\partial \sigma_{zz}}{\partial z} - \frac{\partial p}{\partial z} \right) - \rho g \quad (2.18)$$

The mass balance is shown in equation 2.19

$$\frac{\partial \rho}{\partial t} + \frac{\partial \rho u}{\partial x} + \frac{\partial \rho v}{\partial y} + \frac{\partial \rho w}{\partial z} = 0 \quad (2.19)$$

Equation 2.19 (Roelvink and Reniers (2012)). In these two equations the velocities in x, y and z directions in Cartesian coordinates are given in u, v and w, water density are given as ρ , normal stress is σ and shear stress is τ related to the viscosity, p is the pressure and f_{cor} is the coriolis force. The shallow water equations given in 2.3.1, 2.17, 2.18 and 2.19 are valid for all types of flow and are represented in 3D, 3D is important in areas where there are large variations in over the vertical for example where it is strong density gradients. When this is not the case depth-averaged shallow water equations can be used. This equation is given in 2.20 and 2.21 (Roelvink and Reniers, 2010). These shallow water equations are used in numerical modeling of coastal hydrodynamics and are important for solving coastal problems.

$$\frac{\partial U}{\partial t} + U \frac{\partial U}{\partial x} + V \frac{\partial U}{\partial y} - f_{cor} V = \frac{\partial}{\partial x} D_h \frac{\partial U}{\partial x} + \frac{\partial}{\partial y} D_h \frac{\partial U}{\partial x} + \frac{\tau_{sx}}{\rho h} - \frac{\tau_{bx}}{\rho h} - \frac{1}{\rho} \frac{\partial p_a}{\partial x} - g \frac{\partial \eta}{\partial x} + \frac{F_x}{\rho h} \quad (2.20)$$

$$\frac{\partial V}{\partial t} + U \frac{\partial V}{\partial x} + V \frac{\partial V}{\partial y} + f_{cor} U = \frac{\partial}{\partial x} D_h \frac{\partial V}{\partial x} + \frac{\partial}{\partial y} D_h \frac{\partial V}{\partial y} + \frac{\tau_{sy}}{\rho h} - \frac{\tau_{by}}{\rho h} - \frac{1}{\rho} \frac{\partial p_a}{\partial y} g \frac{\partial \eta}{\partial y} \frac{F_y}{\rho h} \quad (2.21)$$

In the two equations 2.20 and 2.21 the depth and wave average flow including the volumetric transport due to Stokes drift are represented by U and V (depth average flow). f_{cor} is the Coriolis force, D_h is the depth averaged horizontal turbulence viscosity. τ_s and τ_b represents surface and bed shear stress in x and y direction indicated.

Bed shear stress is an important parameter when looking at sediment transport and it arises from the currents and the orbital motions of the water particles (Fredsoe and Deigaard (1992)). The bed shear stress τ_b is shown in equation 2.22, where f_w is the friction coefficient and depend on the local materials and the profile of the coast. This is a part of the shallow water equations but given as parameters for suspended load transport and bed load transport.

$$\tau_b = \frac{1}{2} \rho f_w |\vec{u}| \vec{u} \quad (2.22)$$

2.4 Sediment Transport

The hydrodynamics from previous sections are the main assumptions behind the results off coastal morphology. Coastal morphology is one of the most important design criteria in coastal areas. The coastline morphology is constantly changing due to wave actions and currents and is affecting the usage of our coastal areas.

It can be found many different types of coastal areas; sandy beaches, rocky coastlines and cliffs of different characteristics. All these different types of coastlines will be affected in different ways and the changes takes different time.

The definition of sediment transport is sediments being moved parallel to the shoreline or perpendicular to the shoreline, the sediment can deposit at some locations and eroded at other locations. These two directions are called cross shore sediment transport and long shore sediment transport and the sediment transport at a location is usually a combination of them both.

Sediment transport is dependent on a lot of factors like bathymetry, grain size, fall velocity, density, bed shear stress and energy from waves. An important factor for sediment transport is bed shear stress and is given in Equation 2.22 and the properties of the sediments, and are usually divided into two subgroups called bed load and suspended load sediment transport. It is often a combination of bed load transport and suspended load transport, this depend on the motion of the water and the properties of the sediments. Bed load transport can cause rapid sediment transport because larger stones are moved, in suspended load transport the sediments are floating in the water and sediment transport of this type will not change the morphology as rapid as bed load transport.

2.4.1 Sediment Properties

There are a lot of different sediments that can be found along the shoreline. It is normal to find sediments like clay, pebbles, cobbles sand and gravel in coastal areas. The properties of these sediments are important to find the sediment transport rate. The important factors of the sediments are density, porosity, fall velocity, size etc. These factors are important to evaluate the mechanisms of sediment transport. It is two types of sediment transport bed load transport and suspended load transport, it is two different types but it is normal to have a combination of them.

The fall velocity is shown in Equation 2.23 and is defined by the relationship between the drag coefficient and the gravitational force, both acting in the opposite direction of each other. Fall velocity is the free fall velocity of sediment in clear, undisturbed water. The fall velocity depends on the size, density, shape and roughness of the particle.(Swamee and Ojha (1991)).

$$\omega_s = \sqrt{\frac{4(s-1)gD_n}{3C_D}} \quad (2.23)$$

In the equation 2.23(Fredsøe and Deigaard (1992)) giving the fall velocity, s is the ratio of mass densities of the soil and the fluid, g is the gravity, C_D is the drag coefficient depending on the grain Reynolds number and D_n is the shape factor of the sediments. The other parameters of the sediment can be determined by laboratory investigations.

The critical shields parameter given in equation 2.24 gives the boundary between when sediment transport is occurring and when sediment transport is not occurring. The critical shields stress and with Shields diagram in Figure 2.7 the sediment transport can be found. The shields diagram represents two outcomes sediment transport if the result of the critical shields parameter and the Reynolds number is above shields curve and no sediment transport if it is below. This shields diagram is found from experimental data(Wiki (2016)).

In equation 2.24(Fredsøe and Deigaard (1992)) $\theta_{cr,n}$ is the critical shields parameter, $\tau_{cr,n}$ is the critical bed shear stress, g is the gravity, d_n is the grain size, ρ is the density of the water and ρ_s is the density of the sediments.

$$\theta_{cr,n} = \frac{\tau_{cr,n}}{gd_n(\rho_s - \rho)} \quad (2.24)$$

2.4.2 Bed load Transport

Bed load transport is one of the two types of sediment transport in the coastal zone. It is defined by when sediments are moved by wave and currents in a thin layer along the

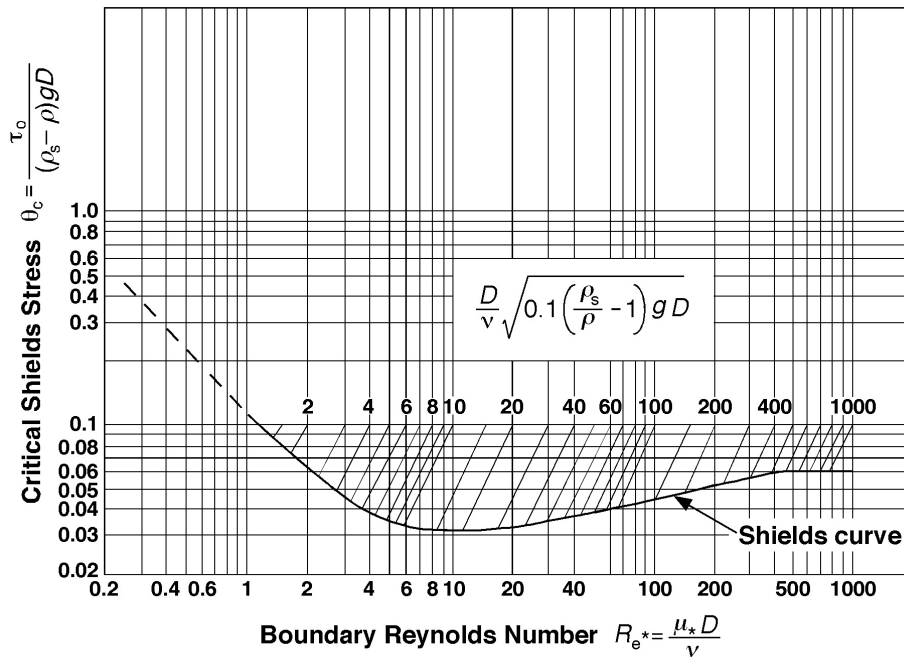


Figure 2.7: Shields Diagram(MIT, 2015)

seabed, they are either rolling, hopping and gliding along the seabed(van Rijn (1984)). This type of sediment transport depends on the bed shear stress and the relationship between bed shear stress and sediment grain size shown in 2.25 and equation 2.26(Fredsøe and Deigaard (1992)).

When the forces on a sediment particle exceed the stability forces and it is these forces that causes the sediment particles to glide, jump or roll over the seabed. Bed load transport is most common when sediments are large and have large densities so the energy of the waves are too small to lift them up. This causes movement close to the seabed.

In equation 2.25 and 2.26 q_B is the rate of bed load transport in volume over time and width, s is the relationship between density of water and sediment, g is the gravity and d is the diameter of the sediments. θ' is the effective shields parameter, Φ_B is the non-dimensional form of bed load discharge(Fredsøe and Deigaard (1992)). Here the difference between critical shields parameter and effective shields parameter gives the rate of sediment transport that can occur. This equation yields for a uniform flow on a plane bed, so it is made some simplifications in these equations. This means that waves are not included in the equations, but they will also have an impact when they make turbulence and swirl up sediments.

$$\Phi_B = \frac{q_B}{\sqrt{(s-1)gd^3}} \quad (2.25)$$

$$\theta' = \frac{\tau'_b}{\rho g(s-1)d} \quad (2.26)$$

When the shield parameter reaches its critical value bed load transport and entrainment begins. This is because the critical bed shear stress is exceeded. Entrainment is when sediments are loosened because of the turbulence close to the sea bottom and brought in to suspended material (Pengsheng Wei and Burnham (2014)). The sediment in suspension will be transported with suspended load transport as described below.

Equation 2.25 and equation 2.26 gives the equations to calculate the bed load transport. When using this equation it is important that the sediments eroded equals the sediments deposited when looking over the total change of an area.

2.4.3 Suspended Load Transport

Suspended load transport is the other type of sediment transport and if suspended load transport is present bed load transport will also be present (Pawe Rowinski (2014)). Suspended load transport is when the particles is not in contact with the seabed for a long period of time. The sediments are floating in the water without being in contact with the seabed. But there is no clear boundary between suspended load and bed load transport, it is therefor some particles that touches the seabed over the distance traveled and some particles are in total suspension (Pawe Rowinski (2014)). Sediments in suspension are often small since they have to be lifted up by the moving water. If the sediments fall velocity are weaker than the turbulence created by the waves the sediments will be in suspension and move with the currents (Pawe Rowinski (2014)). With higher turbulence more particles are in suspension and lower turbulence less particles are in suspension, the water does then have a maximum limit of sediments it is able to have in suspension. This type of sediment transport is not instantaneously affected by motions in the water (Roelvink and Reniers (2012)). This is therefor a slower erosion mechanism than bed load transport and bed load is more critical and can move large amount of sediments in shorter periods.

Suspended materials can be found in the entire water column and a distribution of sediments depended on their properties. The suspension of material have an equilibrium volume of sediments, and when the flow is accelerating the concentrations tends to be lower than for equilibrium flow conditions. It is lower for accelerating flow because sediments need to be lifted up in suspension by turbulence.

Sediment transport is dependent on many factors and has a behavior that is not easily described by formulas. Sediments in suspension can be shown by the following equation that gives the concentration distribution over the height and is here showing the changing:

$$\frac{\partial c}{\partial t} + u \frac{\partial c}{\partial x} + v \frac{\partial c}{\partial y} + (w - w_s) \frac{\partial c}{\partial z} - \frac{\partial}{\partial z} (\epsilon_s \frac{dc}{dz}) - \frac{\partial}{\partial x} (\epsilon_h \frac{\partial c}{\partial x}) - \frac{\partial}{\partial y} (\epsilon \frac{dc}{dy}) = 0 \quad (2.27)$$

In equation 2.27(Roelvink and Reniers (2012)) ϵ_v and ϵ_{psilon_h} is the vertical and horizontal dispersion relation, c is the concentration of sediments in suspension, u and v is the velocity in x and y direction, w_s is the fall velocity. Equation 2.27 is given the concentration over the height The concentrations will also be different for different height over the seabed, but often this is not the most important knowledge needed when investigating erosion of the coastline. Sediment transport in the horizontal is more important for coastline engineering problems. Horizontal variations in sediment concentrations can be found by using Equation 2.28, this equation takes the average over the depth from equation 2.27.

$$\frac{\partial h\bar{c}}{\partial t} + \bar{u} \frac{\partial h\bar{c}}{\partial x} + \bar{v} \frac{\partial h\bar{c}}{\partial y} - \frac{\partial}{\partial x} (\epsilon_h \frac{\partial h\bar{c}}{\partial x}) - \frac{\partial}{\partial y} (\epsilon_h \frac{\partial h\bar{c}}{\partial y}) = \frac{h(\bar{c}_e q - \bar{c})}{T_s} \quad (2.28)$$

In equation 2.28(Roelvink and Reniers (2012)) T_s is the timescale and $\bar{c}_e q$ is the equilibrium depth-average concentration and \bar{c} is the average concentration.

2.4.4 Soulsby-Van Rijn Formula

Soulsby-van Rijn formula is a set of formulas calculation sediment transport in coastal areas. The formulas from van Rijn are preferable because they calculates suspended and bed load transport separately, the wave and current combination are included and the bed slope is included(Rolvink and Reiners, 2010). ζ is a general multiplication factor calculated by currents and waves, A_{sb} and A_{ss} is the bed load and suspension load multiplication factor taking into account sediment diameter(D_{50}), water depth(h), gravity(g), density of water(ρ) and particles(ρ_s) and kinematic viscosity(μ). The sets of equations below will give the sediment transport when investigating a locations with both waves and currents(Roelvink and Reniers (2012)).

$$\begin{aligned} S_b x &= A_{cal} A_{sb} u \zeta \\ S_b y &= A_{cal} A_{sb} v \zeta \\ S_s x &= A_{cal} A_{ss} u \zeta \\ S_s y &= A_{cal} A_{ss} v \zeta \end{aligned} \quad (2.29)$$

$$A_{sb} = 0.05h \left(\frac{D_{50}/h}{\Delta g D_{50}} \right)^{1.2} \quad (2.30)$$

$$A_{sb} = 0.012D_{50} \frac{D_*^{-0.6}}{(\Delta g D_{50})^{1.2}} \quad (2.31)$$

$$D_* = \left[\frac{g\Delta}{\mu^2} \right]^{1/3} \quad (2.32)$$

$$\zeta = \left(\sqrt{u^2 + v^2 + \frac{0.018}{C_f} U_{rms}^2} - U_{cr} \right)^{2.4} \quad (2.33)$$

$$U_{cr} = \begin{cases} 0.19D_{50}^{0.1} \log_{10}(4h/D_{90}) & D_{50} \geq 0.5mm \\ 8.5D_{50}^{0.6} \log_{10}4h/D_{90} & D_{50} \leq 2mm \end{cases}$$

2.5 Morphological Processes

Morphological processes describe behavior of the processes that are changing the coastal areas. Sediment transport is an important part together with changing water depth. When all processes are included it will be a system of sediment transport, waves, currents and bottom changes. Equation 2.35(Roelvink and Reniers (2012)) gives the relationship between bed load transport in both the x and y directions and the changing water depth(z_b). This should be equal to deposition and erosion in the coastal area that are investigated.

$$(1 - \epsilon) \frac{\partial z_b}{\partial t} + \frac{\partial S_{bx}}{\partial x} + \frac{\partial S_{by}}{\partial y} = D - E \quad (2.35)$$

Equation 2.35 describes how the sediment transport in x and y direction is changing and the relationship with how the relationship between deposition and erosion is. Over an area deposition must be equal to erosion and therefor equation 2.35 can be rewritten as equation 2.36. In these two equations E is erosion, D is deposition, S_x and S_y is the sediment transport in x and y direction(Roelvink and Reniers (2012)).

$$(1 - \epsilon) \frac{\partial z_b}{\partial t} + \frac{\partial S_x}{\partial x} + \frac{\partial S_y}{\partial y} = 0 \quad (2.36)$$

2.6 Modeling For Coastal Hydrodynamics and Sediment Transport

Many processes take place in the coastal zone described in the previous sections. Numerical modeling is a very useful approach to quantify these processes which help to understand and hopefully predict the behavior of the coast. Cross shore, long shore and a coastal area model, the cross shore model is neglecting. The contribution of long shore changes and long shore models neglects cross shore changes. Coastal area model can model be 2D and 3D. In this thesis a way of modeling the situation at Svalbard in 2015 will be chosen.

Chapter **3**

Arctic coastal erosion

3.1 Introduction

Throughout history the climate has changed constantly and is fluctuation between warm and cold temperatures. The average temperature can change over several year and the temperature is changing over the year. The trend the recent years is that the average temperature is increasing among with other environmental changes(NASA (2016b)). The Climate change is also changing other factors than just an increase in temperature, sea water level is rising, glaciers are melting, snow and ice is retreating in our Arctic areas and water temperature is increasing. (NASA (2016b))(NASA (2016a)). All of these factors are changing the dynamics of the arctic environment.

The erosion rate in the arctic is considered as one of the highest in the world(B. M. Jones and Flint (2009)). Every year several meters of soil will erode and this erosion rate is increasing(B. M. Jones and Flint (2009)). Because of this change the climate change is a problem in higher latitudes and need investigation. In higher latitude the coastal zone is the area where human activities are located(Volker Rachold (2004)). The actions in Arctic coastal zones are variable and depend on factors like wind, waves, tides, currents, temperature, ice concentration, sea level changes and properties of ground material(Volker Rachold (2004)).

During the winter months the Arctic areas are covered by ice and the coastal zone is protected by wave actions because they are not able to reach the shoreline(B. M. Jones and Flint (2009)). When the temperature is rising, the coastline is experiencing longer ice free periods. This changes in the arctic environments is why thermal properties are important. In addition to the increase in temperature and lack of ice the number of extreme events and the intensity of the storms will increase(Martin Beniston and Woth (2007)).

Because of the changing of the environment in the coastal zone, it is desirable to investigate the coastal areas. The investigation will help to be able to predict storm events and their outcome to be able to protect infrastructure, economical value and human lives.

Further in this chapter the mechanisms causing coastal erosion in the Arctic will be described. In addition to the mechanisms described later in this section the arctic is experiencing large erosion rated because of melting snow in the spring(Gugan and Christiansen (2016b)). When the snow and ice is melting on land it erodes away sediments. This type of erosion is not important for this thesis because it is considering a storm in September when all snow and ice is melted.

3.2 Thermal Erosion Processes

In the Arctic there are new types of mechanisms occurring regarding coastal erosion. There are mainly two types of erosion mechanisms that are new for the Arctic they called Thermal denudation and thermo abrasion(F. Gunther and Grigoriev (2013)). These two erosion

types depend on different mechanisms and will be described below. The same sediment transport types from temperate areas are happening in the Arctic.

3.2.1 Thermo Denudation

The first type of thermal erosion is called thermal denudation. This mechanism is characterized as when the ice and frozen soil along the shoreline has melted, and the soil loses its strength (F. Gunther and Grigoriev (2013)). The stability of the sediments will be reduced because the soil is melted. The bluff will not be stable enough to stand and it will collapse. With this kind of erosion mechanism the waves are important to transport the sediments that collapses away. Waves can also gradually change the steepness of the coastal profile by removing sediment at the bottom and make the bluff steeper. Due to the decrease of stability when the shoreline reaches a certain steepness the cliff will fail and glide into the water. When the sediment reaches the water the currents and wave actions will transport the sediments away and the process will start over again. The process is illustrated in Figure 3.1.

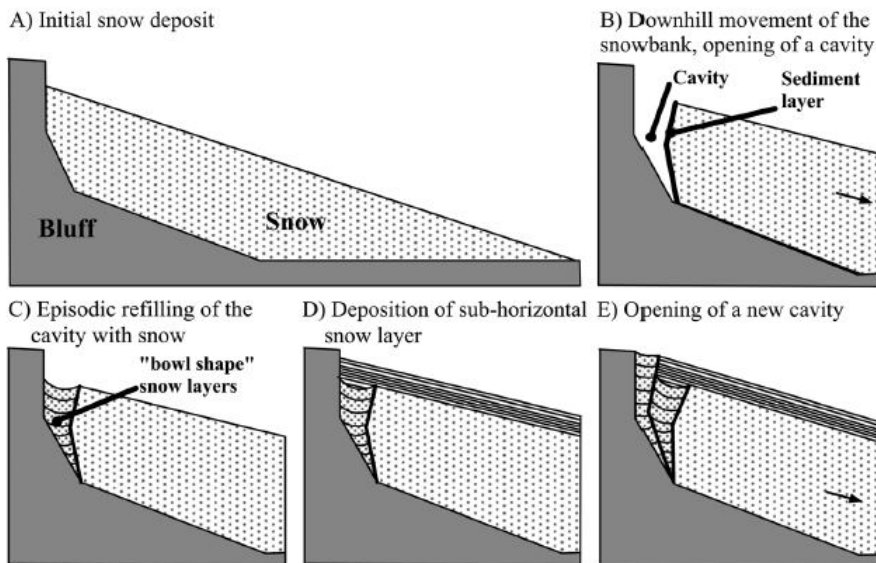


Figure 3.1: Thermo Denudation process (Gugan and Christiansen (2016a))

3.2.2 Thermo Abrasion

The second type of sediment erosion happening in the arctic is thermo abrasion. This type of sediment erosion is happening when the shoreline is exposed to waves and the soil are frozen or contains a lot of ice (Volker Rachold (2004)). Thermo abrasion is a combination of mechanical processes and thermal processes and both of them are important to find the rate of erosion (F. Gunther and Grigoriev (2013))(?). The waves will have a higher temperature than the frozen soil and is therefore able to melt the fozen soil and possible ice at the shoreline, the melted sediment will then be easier eroded away and the soil that is melted. Waves interact with the toe of a cliff melting the frozen soil and make a notch. The waves will extend and widen this notch to a crack with a cliff of frozen soil above, when this crack deep enough the cliff will get to unstable and collapse (Volker Rachold (2004)). The waves will still be interacting with the shore face and remove sediments either offshore or currents transport the sediments along the shore to deposit it or it will be taken off shore from another location. This type of Arctic erosion is shown in Figure 3.2

Thermal abrasion is not happening constantly and are an uneven mechanism, when the cliff collapses huge amount of sediment disappear in a fast rate. This type of erosion can vary a lot from year to year. The evolution of the crack can take several years, but when the soil gets unstable and collapse the erosion is fast. Thermal abrasion is often happening when there are a storm surge present, so if there is just moderate wave condition thermal abrasion not so likely to happen.

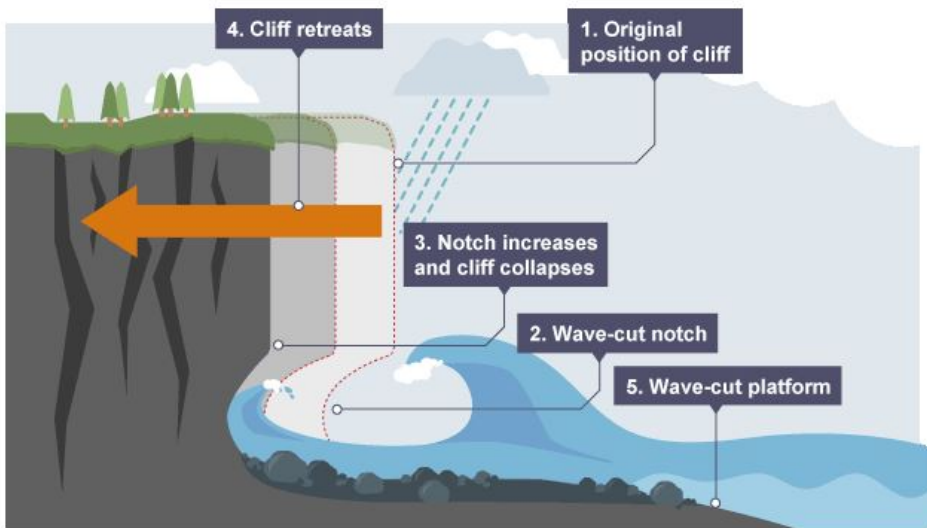


Figure 3.2: Description of thermal abrasion process (BBC (2016))

Chapter **4**

Numerical Modeling

4.1 Introduction

4.2 MIKE21

This section will describe MIKE21 by DHI, which is a numerical modeling tool used for offshore, coastal and marine engineering problems. It will be used for running the numerical simulations in this thesis. It can be used in design of harbours and bridges over water, coastal protection, environmental impact, flooding and storm surge investigation, etc. (DHI (2015))

MIKE21 is a 2D program modeling non-linear behavior of the hydrodynamics. Another program developed by DHI is MIKE3 and this is a 3D modeling program. For this thesis only the coastal part of the program will be described. The parts of MIKE21 that will be used is MIKE21 Flow HD and MIKE21 SW. Due to time limitations MIKE21 ST is not used in this thesis. The assumptions behind MIKE21 is incompressible Reynolds averaged Navier-Stokes equations, hydrostatic pressure and Boussinesq equation. To get a reliable answer the model is also including equations regarding salinity, temperature, continuity, momentum, turbulence and density of water.

The applications included in MIKE21 is flow HD, Spectral Wave(SW), Boussinesq Waves (BW), Elliptic Mild Slope Waves (EMS), Parabolic Mild Slope Waves (PMS), Non-Cohesive Sediment Transport (ST), Mud Transport module(MT) etc. For this thesis MIKE21 Flow HD and MIKE21 SW will be used. MIKE21 SD was supposed to be used, but this will be recommended as further work.

4.2.1 MIKE21 Flow Hydrodynamic (HD)

MIKE21 is an advanced numerical tool for modeling coastal hydrodynamics. The program can be used for most coastal and marine approaches, both in the sea, bays, estuaries and in lakes. Since this is a complex program that requires a lot of parameters. At the same time it can provide a more realistic presentation of the natural conditions.

MIKE21 is a non linear program based on numerical solutions using shallow water equations in 2D, with the assumptions of incompressible depth-average Reynolds Navier-stokes equations(group (2016a)). Within the model it includes salinity, temperature, momentum and continuity equations.

MIKE21 include a lot of parameters in their simulations some of the included features are listed below(group (2016a))

- Momentum dispersion
- Bottom shear stress
- Coriolis force

- Wind shear stress
- Barometric pressure gradients
- Ice coverage
- Tidal potential
- Tidal precipitation/evaporation
- Wave radiation stresses
- Sources and sinks

4.2.2 MIKE21 Spectral Waves (SW)

MIKE21 SW is the spectral wind wave modeling application within MIKE21, modeling locally generated wind waves and swell in offshore areas to find the conditions at the site of interest. This is a phase average application and a detailed description of the waves behavior will not be provided using this application(group (2016b)). It simulates the growth, decay and transformation of wind generated waves. The application solves wave action conservation equations that is based on parametrization, where each element is described by a two dimensional wave action spectrum. Many important physical phenomena is included in the modeling of the waves, for example, dissipation due to white-capping, bottom friction and depth-induced wave breaking, refraction and shoaling, wave current, non-linear wave interaction, wave growth because of wind and the effect of varying water depth(group (2016b)).

This application is useful in near-shore and offshore areas when the information that is needed is more general in significant wave height, wave period, energy, magnitudes of currents etc. If the waves are generated in an offshore position and travelling to a near-shore it is useful to use a flexible mesh which is also provided in this application. A coarser mesh can be used offshore and a finer mesh can be used closer to the point of interest. Therefore a higher resolution of result in point of interest can be provided. The output of this application will be used in other application to calculate the sediment transport.

Required input for this model is bathymetry and a mesh over the area that are going to be modelled. Wind forcing is another input parameter and can be given as components in x and y direction varying in time and as just varying in time but constant over the domain. The tidal variation will be given as a condition at the boundary.

4.2.3 MIKE21 Sediment Transport (ST)

As stated earlier MIKE21 ST will not be used due to time limitations. MIKE21 ST simulate erosion, deposition and transport of non-cohesive sediments(group (2016c)). The application is suitable for studying sediment problems in near shore or offshore areas.

MIKE21 ST uses results from MIKE21 Flow HD and MIKE21 SW.

Included parameters:

- Tide
- Wind
- Waves
- currents

Using MIKE21 ST it is possible to calculate sediment transport using two different approaches. Number one only includes currents and the second includes waves and currents (group (2016c)). In this thesis it is the approach where waves and currents are included that are important and pure currents will not be discussed.

Below is a list of the properties in MIKE21 ST (group (2016c))

- Constant or spatially varying bed material
- Two simulation methods are available:
 - Deterministic intra-wave sediment transport model STP (Application from DHI)
 - Bijker's total-load transport method.
- The STP model provide these features to MIKE 21 ST:
 - Arbitrary direction of wave propagation in respect to the current
 - Distinguish between breaking and unbroken waves
 - Geometric properties of bed material is described through a single grain size or a grain size distribution curve
 - Plane/ripple-covered bed
- Courant-Friedrichs-Lewy stability criterion

Case study

5.1 Introduction

For this thesis Bjørndalen at Spitsbergen is chosen as case study. The location is shown in Figure 5.1. From 29th to 30th of September 2015 there was a major storm that caused large coastal erosion at Bjørndalen. Bjørndalen is located between Longerbyen and Barentsburg and is a popular area for cabins. After the storm these cabins were very close to the seafront and only centimetres from the cliff leading to the sea(Barstein (2015)).

There are no measuring stations at Bjørndalen, but both at Barentsburg and at Svalbard airport have measuring stations. In this case study MIKE21 by DHI is going to be used to model the storm conditions at Bjørndalen during the storm in 2015. Wind data are taken from the measuring stations to Norwegian Meteorological Institute(NMI) and numerical simulated wind values from European Centre for Medium-Range Weather Forecasts(ECMWF).

During long periods of the year Bjørndalen is covered by sea ice and protected by it. Because of the climate change and increasing temperatures the ice free periods in the Arctic are decreasing. The Arctic areas are more exposed now than ever because of the combination of increasing storm events, increasing intensity of the storm and longer ice-free periods(NASA (2016a)). Arctic coastal zones is important for the connection between the sea and land, it is important to be able to predict and protect coastal areas in the Arctic(Donald L. Forbes (2010)).

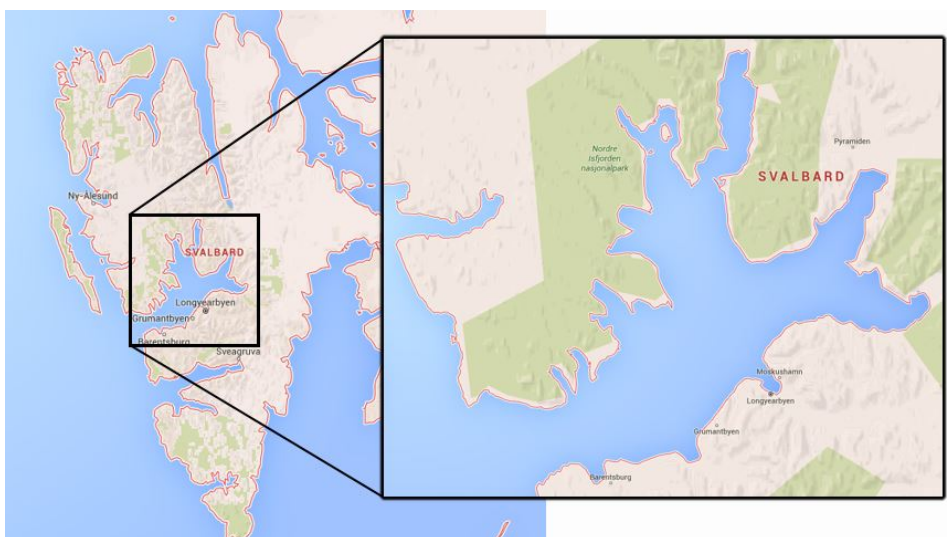


Figure 5.1: Area map showing the location of Bjørndalen at Isfjorden on Svalbard

5.2 Description of Area

The landforms at Svalbard are created by various geological processes, more precisely tectonic uplift followed by denudation(et Al (2009)). When parts of the land are ice free, permafrost is present. With climate change the permafrost is also decreasing during the icefree periods and leads to a decrease in stability for the ground materials.

During the last ice age Svalbard was covered by glaciers and the sea water level was 130m below the sea water level today(et Al (2009)). But still Marine sediments are found at Svalbard, the reason for this is that the ice was pushing the land down under the marine boundary and when the ice melted the land was left under water and started to rise[et Al (2009)]. As the land is rising marine sediments are showing up over the surface. The land rising is happening at the same time as global climate change is increasing the water level, due to the effect that water level increasing all over the world, Svalbard is experiencing that the land is rising more than the water level(et Al (2009)). Svalbard is experiencing that the beach zone becomes larger. This entire paragraph is described in (et Al (2009)).

The sediments in Bjørndalen is mainly marine sediments like sand, gravel and stones are to be found up to 60-70 m above the sea level today(et Al (2009)). It is hard to predict the exact marine limit because of several processes that have changed the area. Marine depositions have caused scattered terraced shapes combined with steep sides going down to the sea. These landscape profiles looks like cliffs hanging over the shoreline. (et Al (2009))

5.2.1 Bathymetry

The Bathymetry data for Isfjorden is shown in figure 5.2. Here the green line represents the boundary where the offshore conditions will be applied. The depth in the middle of Isfjorden is the deepest and goes down to 375m below the water surface. The bathymetry of Bjørndalen is provided by Jeppesen (2015)).

Land and water depth is given in two different files. First the shoreline is smoothed out so MIKE21 by DHI will be able to run the simulations without any complications. When the shoreline is smoothed the water depths are applied and smoothed to fit the shoreline and match into the system. The next step is to generate a mesh, this mesh is coarse in Isfjorden with a finer mesh around Bjørndalen. This modification of the mesh is chosen to get a higher resolution of the modeling data close to the site of interest. Using this type of mesh during all processes when modeling will strengthen the results.

Since Bjørndalen is a large area all small islands away from Bjørndalen are removed to minimize the complexity of the area. In addition the small fjords are smoothed more and some are removed from the mesh, this is also done to minimize the complexity of the mesh since the area is fairly large.

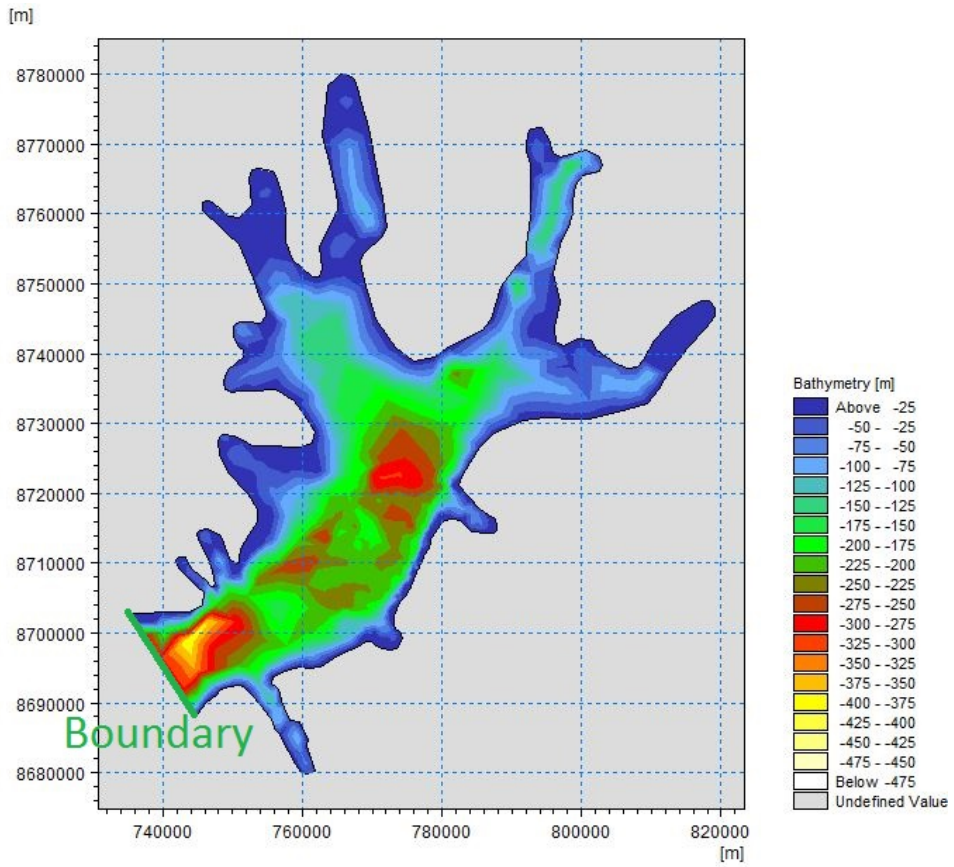


Figure 5.2: Isfjorden bathymetry for MIKE C-MAP

5.2.2 Wind

For local wind generated waves, the wind speed and direction play an important role in the making. There are three local measuring stations at Svalbard close to Bjørndalen. The measuring stations are Isfjorden Radio station, Barentsburg and at Svalbard Airport. From these measuring stations, the values for average wind and maximum wind are calculated for 2015. The average wind speed for the three measuring stations is 6.22 m/s and the maximum measured wind speed is 26.5m/s. The average wind for the storm in September is 8.46m/s (calculated for only 29-30 September using data from NMI). Wind data from NMI is given for every hour and the value given is the average of one hour. The wind data that are measured are measured at different heights for the three locations. The wind velocity is corrected using Equation 5.1(S. A. Hsu and Gilhousen (1994))to have the wind given at 10m height above sea level. In the Equation u_2 is wind speed at height z_2 , u_1 is wind speed at height z_1 . u_1 and z_1 are known. The P used in this case is 1/7.

Wind data for Isfjorden were also collected from European Medium-Range Weather forecast database(EMCWF)(forecast database (ECMWF)). This is a wind field that gives the wind in components of u and v, representing the wind speed in north and east direction. The spacing between the data points is 0.125° . The data is given for every 6 hour where the value represented is the average of 30 minutes. These values are modeled values for the wind. The data is for wind at 10m above sea level.

Wind data for 2015, direction and speed are taken out from the ECMWF data set to be compared with NMI data. The wind is then taken out at the same location as the measuring stations. The comparison of the velocities are shown in Figures 5.3, 5.4 and 5.5 and in Tables 5.1 and 5.2. The s for NMI and ECMWF are shown in Figures 5.6, 5.8 and 5.7. From the Figures 5.3, 5.4 and 5.5 there are possible to see that the wind is following the same trend, there are no major differences in the wind speed behaviors and they behave in the same order. Looking at the tables the average wind velocity from NMI is higher for all the three locations. The two graphs showing wind from NMI and ECMWF are not showing the exact same results given the sampling of the wind is different for NMI and ECMWF. The direction for the measured wind and the wind modeled by ECMWF has few similarities and they are not blowing in the same direction. When the wind is adjusted with power law the mean value difference is increasing for Isfjorden radio station and Barentsburg. The mean wind speed difference for Svalbard airport is decreasing.

The advantages of using wind from NMI are that the data are accurate and it gives the correct velocity and the correct speed. However, the wind speed at the three locations are different and a good representation of the wind conditions over Isfjorden using any of these. The advantages of using wind data from ECMWF is that it will give a realistic description of how the wind is behaving over an area at Bjørndalen. The wind has a lower mean value and the directions are hard to compare with each other. but this wind field will give a better representation of how it will be in natural conditions. Further in this thesis and the modeling the wind data from ECMWF will be used. These data is not the best representation of the wind but it is the best data available for Bjørndalen.

$$\frac{u_1}{u_2} = \left(\frac{z_2}{z_1}\right)^P \tag{5.1}$$

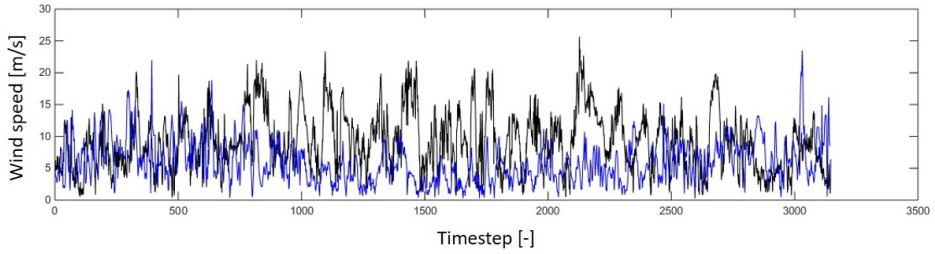


Figure 5.3: Wind speed for Isfjorden Radio, black is NMI and blue is ECMWF

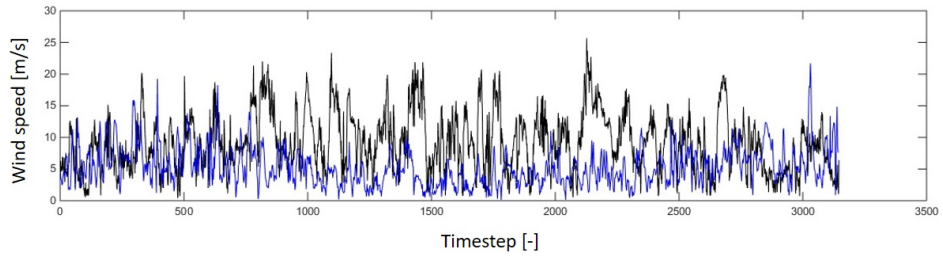


Figure 5.4: Wind speed for Barentsburg, black is NMI and blue is ECMWF

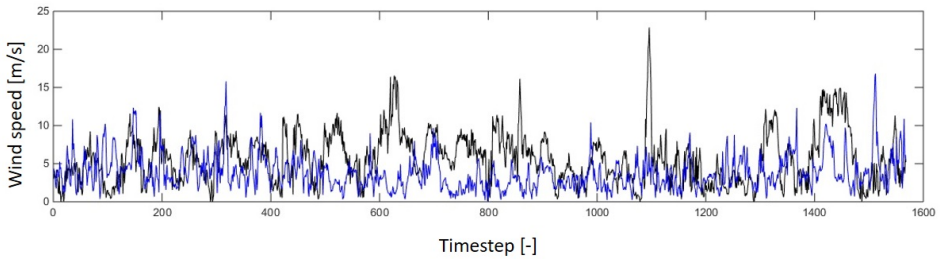


Figure 5.5: Wind speed for Svalbard Airport, black is NMI and blue is ECMWF

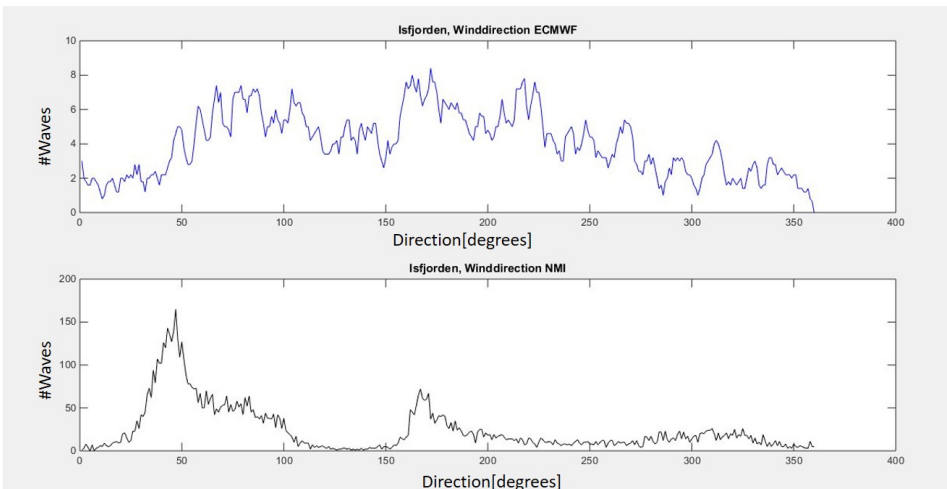


Figure 5.6: Wind direction for Isfjorden radiostation

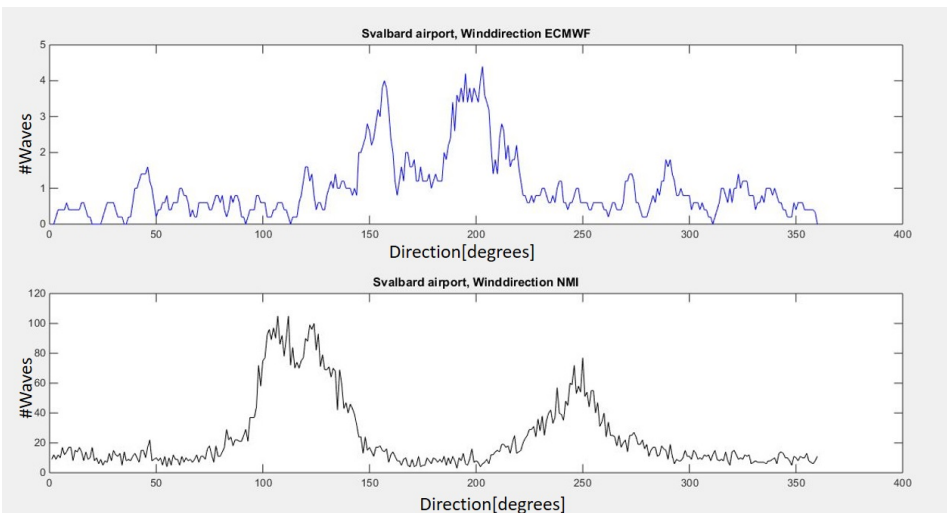


Figure 5.7: Wind direction for Svalbard airport

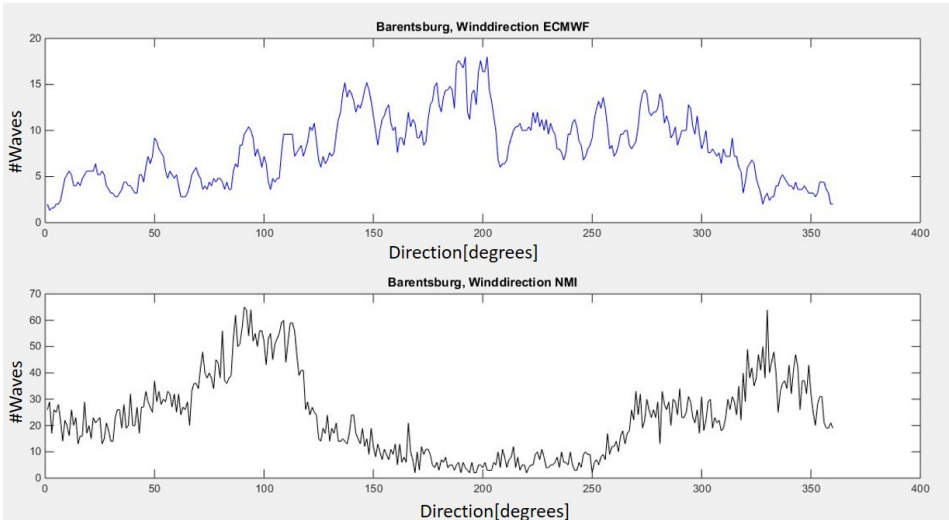


Figure 5.8: Wind direction for Barentsburg

Station	Standard deviation[m/s]	Mean value[m/s]
Isfjorden NMI	4.56	9.17
Isfjorden EVMWF	3.03	5.93
Svalbard airport NMI	3.35	5.65
Svalbard airport ECMWF	2.22	3.77
Barentsburg NMI	4.56	9.17
Barentsburg ECMWF	2.98	5.31

Table 5.1: Middle Wind speed at Svalbard airport correlated for measurement height using power law

Station	Standard deviation[m/s]	Mean value[m/s]
Isfjorden NMI	4.33	8.71
Isfjorden EVMWF	3.03	5.93
Svalbard airport NMI	3.89	6.54
Svalbard airport ECMWF	2.22	3.77
Barentsburg NMI	4.33	8.72
Barentsburg ECMWF	2.98	5.32

Table 5.2: Middle Wind speed at Svalbard airport without correlation for measured height

5.2.3 Waves

At Svalbard and the area around there are no hindcast data available. Neither any locations close to Svalbard has available data. The waves that will be included for this site are modeled by NMI using offshore wind data to model the waves entering Isfjorden. Data for September and October are modeled for three locations at the boundary of Isfjorden. There is no way to verify this wave data and trust in the model of NMI is needed. The modeled data are shown in Figure 5.10

The wave data from NMI is given as a grid size of 10kmx10km, given every third hour calculated from wind averaged over one hour. This is a coarse wave profile and not very accurate, but it is the best data available. As input in MIKE21 SW the wave data is given as parameters and not as waves varying over time, therefore the accuracy of the wind and the grid may not be so important.

The main direction of the most energetic wind waves entering Isfjorden comes from a direction of 180-250 degrees. The direction is given from the north, in coastal degrees. 180-250 degrees represents south west direction. A visual representation of the waves is given in Figure 5.9. The parameters calculated from the wave data modeled by NMI are $H_s = 3.3\text{m}$, $T_p = 13.3\text{s}$ and the main direction is 223 degrees with standard deviation of 5 degrees.

Figure 5.10 shows the significant wave height for the swell entering Isfjorden modeled by NMI. Here the maximum significant wave height H_s is 4.25m. And it is occurring during the storm. The significant is calculated as the mean of the significant wave height occurring at the site.

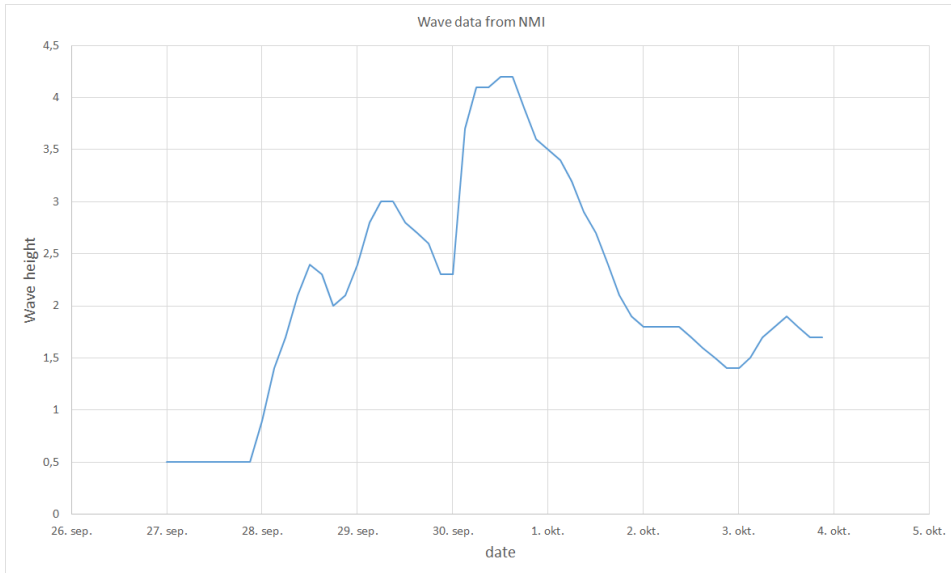


Figure 5.9: Wave height for the wave conditions modeled by NMI

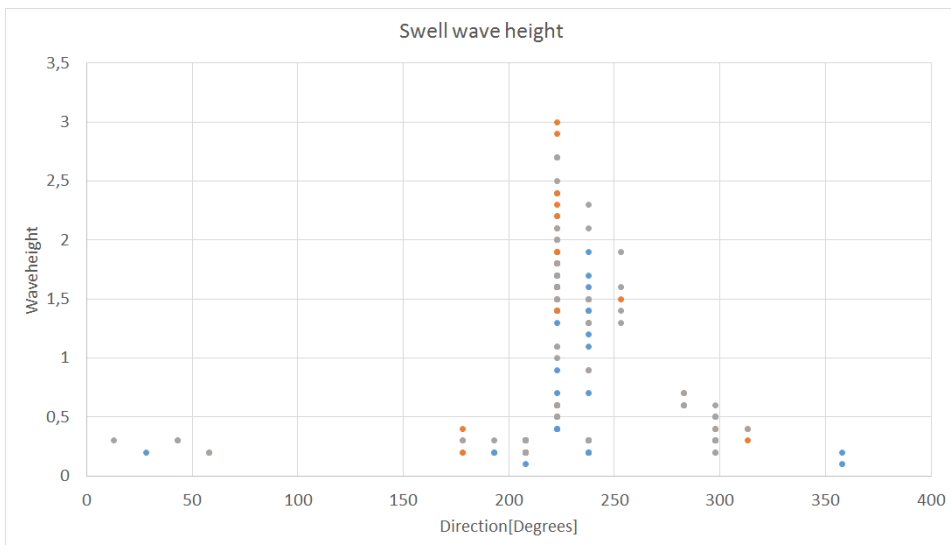


Figure 5.10: Swell wave height over direction for 27 September to 4 October

5.2.4 Water level

The water level at a site is mainly dependent on the tides at the area. There are no measurements at Svalbard from NMI, the tides are therefor collected from(Jeppesen (2015)). The tides used from C-Map is represented in Figure 5.11, the figure is showing how the water level is varying from mean sea level. The difference is approximately 1.8m.

In figure 5.12 the water elevation in Hammerfest, Finnmark is shown. This is the closest available measurements of water level and is included to compare the water level in Isfjorden with water level in Hammerfest. The difference of high and low tide in Hammerfest is approximately 3.3m.

Since the water level fluctuation in Hammerfest is 3.3m and the water elevation in Isfjorden is 1.8 it gives confidence in the water elevation at Bjørndalen.

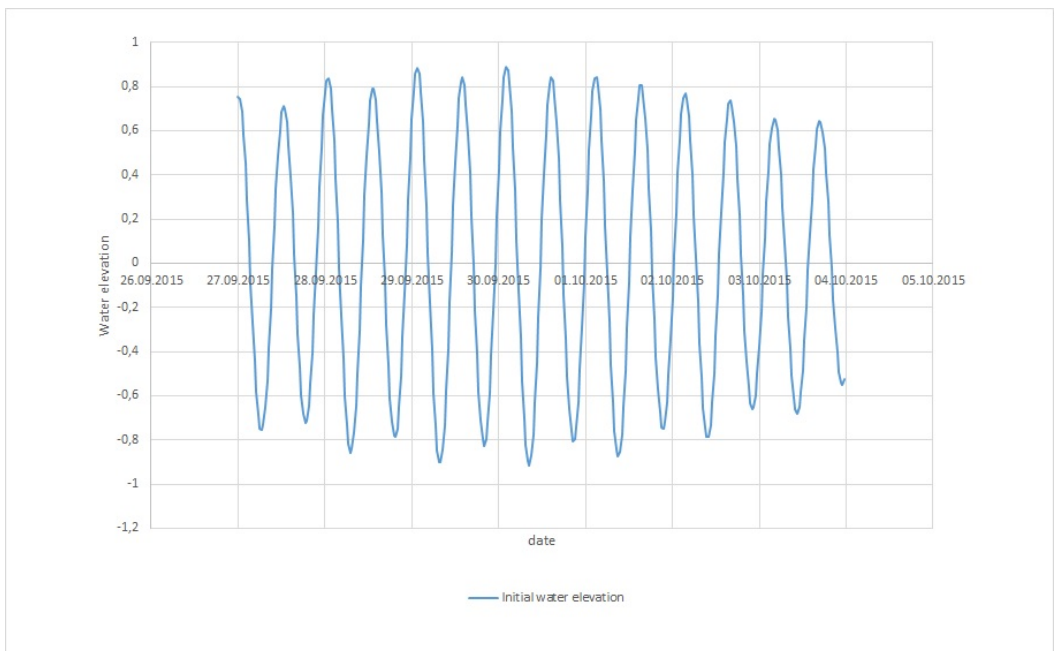


Figure 5.11: Water elevation at Bjørndalen

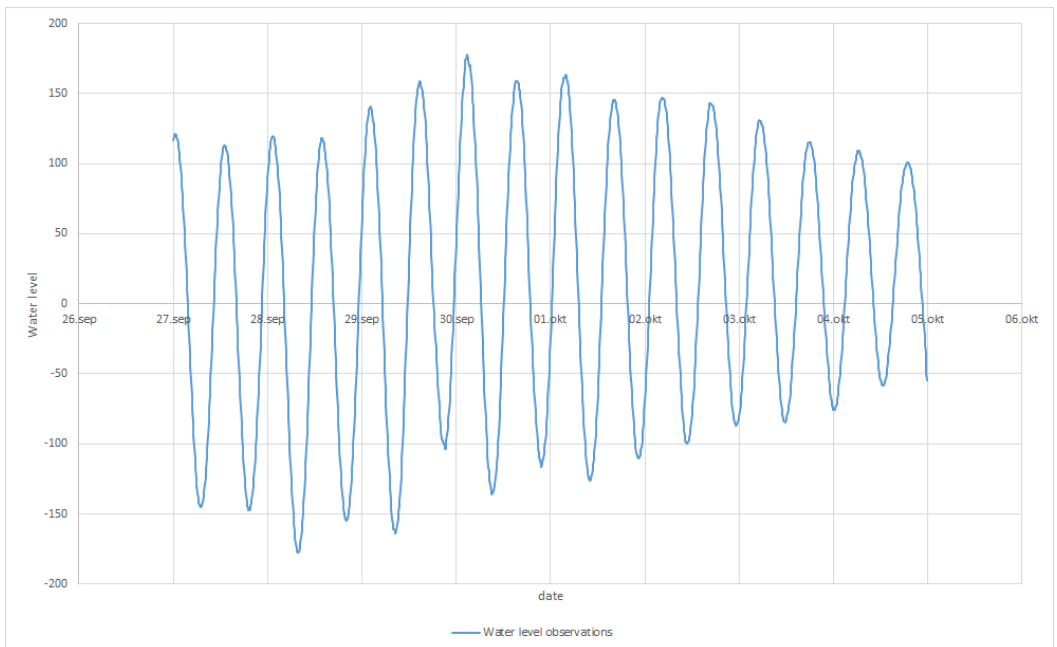


Figure 5.12: Water elevation at Hammerfest in Finnmark, Norway

5.2.5 Sediment properties

There have been done some research at Vestpynten and gathered information about the sediment properties at the area(?). This information about the sediments at Bjørndalen is collected from Vestpynten when assuming almost the same properties of sediments are present at both locations since they are not far from each other and there is no other available data from Bjørndalen. That this is almost correct can be found by the description of the area in (et Al (2009)). The concentration at Bjørndalen is based on the samples taken at Vestpynten.

5.3 Numerical model setup

Numerical modeling is a well used approach to study for marine environment and to solve coastal engineering problems. There is a large range of different softwares to choose from. Available softwares are commercial and open source. In this thesis MIKE21 by DHI will be used, this is a commercial and state of the art program used all over the world in coastal problems. MIKE21 is used because it is a proven tool for modeling the hydrodynamics in nonArctic environments. Therefor it is desirable to investigate the validation of MIKE21 in Arctic environment. MIKE21 by DHI is a favorable software because it has flexible mesh that allows the user to have a higher accuracy in the area of interest. This application allows the user to have smaller grids at the area of interest and larger grid at areas away from area of interest. This especially good for this thesis when the modeling area is large and the site of interest is much smaller.

MIKE21 by DHI is a 2D modeling program but, is also available in 3D and called MIKE3, in this thesis the 2D program MIKE21 by DHI gives sufficient information about the condition at the site of interest. The applications in MIKE21 are described in chapter 4.

The conditions of the storm that occurred 29th to 30th of September 2015 are investigated using data from 27.09.2015 to 04.10.2015 to simulate the storm conditions. The first step is to use MIKE21 Flow HD by DHI to get a simulation that represents the flow conditions in Isfjorden caused by wind and tides. Step number two is to use the results from MIKE21 HD by DHI in MIKE21 SW by DHI to get information about the wave conditions because of the flow conditions, waves, tides and wind. This model is supposed to give all the important information needed for investigating coastal erosion.

5.3.1 Model Setup for MIKE21 Flow HD

When using MIKE21 Flow the effect of wind and tides are going to be investigated. In this section waves or wave parameters are not included. The model is modeling the flow and hydrodynamic conditions in the entire fjord.

The mesh described above will be used in this simulation. Isfjorden is a large area but the modeling period is short therefor it is possible to have a shorter modeling time step, and this time step is chosen to be 30 sec, an increase in modeling time step would decrease the modeling time. To not use too much time and be able to run enough simulations for this master it is chosen to use low order theory when modeling.

The eddy viscosity and Manning's number is select when using MIKE21 Flow HD. Both of these values are important when modeling small areas and can have an influence on the result. Since the modeling area in this thesis is large the two numbers are chosen to be as default. Manning's number is $m = 32$, and the eddy viscosity coefficient = 0.28. The values are also representable for the area since they depend on the natural conditions.

The tides are included at the boundary at the entrance of Isfjorden. With an initial value of 0 based on the average tidal variation at the boundary. The tides will therefor be modeled for the rest of the area.

Precipitation and evaporation, tidal potential and infiltration are not included in the model. They are not included because of the length of the modeling time, the effect of these will be small and can therefore be neglected.

The Coriolis force is included because it will have some effect on both the wind and currents of such a large area.

Run1: Constant wind data from NMI and tides from C-map

Run2: Varying wind data from ECMWF and tides from C-map

Run3: Constant wind data from NMI, no tides

Run4: Varying wind data from ECMWF, no tides

Run1: Constant Wind Data From NMI and Tides From C-map

The first simulation of the storm event is using wind data from NMI and tides from C-Map collected from Jeppesen charts. The direction and magnitude of the wind from NMI is constant over the domain and varying in time, the chosen wind file used in this simulation is Isfjorden radio station, and this is chosen to be conservative. Water elevation is varying and included in the model as a boundary condition at the entrance of the fjord. The wind field used in this model is the measurements at Isfjorden radio station, this is the data set with highest values and is therefor conservative and may give higher answers than expected.

Run2: Varying Wind Data From ECMWF and Tides From C-map

Simulation number two is done with wind field from ECMWF. ECMWF is a wind and pressure field varying over time and domain where the wind data is given in a x and y component and pressure is given for each grid. The tidal variations are the same as in run number one. This wind field gives a better representation on the behavior of natural processes in the coastal zone. To use varying wind field will give a better representation of the conditions but will be more important for the SW model.

Run3: Constant Wind Data From NMI, No Tides

Simulation number three is modeling without tides to find the effects when only wind is present at the area. The wind data is from NMI and constant over the domain. The same wind field was used in run number one.

Run4: Varying Wind Data From ECMWF, No Tides

Simulation number four is modeling without tides and with wind data from ECMWF is included. Wind data from ECMWF is varying over the domain and in domain. This is the same wind from run number two.

5.3.2 Model Setup for MIKE21 Spectral Wave

After MIKE21 Flow is used to run MIKE21 SW is the next step in getting information about the conditions in Isfjorden. After MIKE21 is run information about the flow conditions, the water elevation and currents. This will be used in MIKE21 SW to get information about the wave conditions in Isfjorden. The properties of the waves, tides, radiation stresses and currents are going to be investigated. These properties are important when investigating coastal erosion and sediment transport.

In MIKE21 SW the results from MIKE21 HD will be used, the output files from MIKE21 Flow HD that will be used are currents velocities, current direction and surface elevation.

Diffraction is not included in this model because diffraction has no relevance for the case study investigated. Breaking wave are included with gamma value of 0.8. Bottom friction is based on the sediment particles size at the site and here it is based on the most coarse layer since the sediments most parts of the time is frozen and will behave like the particles are more coarse. The wave parameters are calculated from wave data modeled by NMI using offshore wind. This information is used as input to the boundary condition and the program is modeling from these values.

MIKE21 SW will be run three times.

Run1: Offshore waves from NMI , varying wind from ECMWF, water elevation and currents from MIKE21 Flow HD

Run2: Varying wind from ECMWF, water elevation and currents from MIKE21 Flow HD

Run3: Offshore waves from NMI, water elevation and currents from MIKE21 Flow HD

The main idea behind these three runs are to evaluate the effect of the input parameters on waves and currents that play an important role in evaluation coastal erosion and sediment transport. It would have been a good idea to also model the conditions in Isfjorden with only wind and wave parameter. In this case the water elevation and currents from MIKE21 Flow HD would not have been taken into consideration and the currents and water elevation of waves would be more visible.

5.3.3 Sediment transport

The next step for this investigation would have been to model the sediment transport due to the natural conditions modeled by MIKE21 Flow HD and MIKE21 SW. Due to the time limit there was not enough time to investigate this part of the problem. The conditions that are important for the sediment transport are the most important to investigate. Bjørndalen is located in an Arctic area and the sediment transport and coastal erosion would have needed to be evaluated and used simplifications within the program. MIKE21 ST application is modeling for Cohesive sediments witch is not the case at Bjørndalen. If numerical modeling with MIKE had not been possible another solution would have been to use a numerical program developed for coastal erosion in the Arctic or cliff erosion in coastal areas.

Results and discussion

6.1 MIKE21 Flow HD

Figure 6.1 shows a map over Isfjorden where the point the results is gathered from is located. The cross in the figure represents this point.

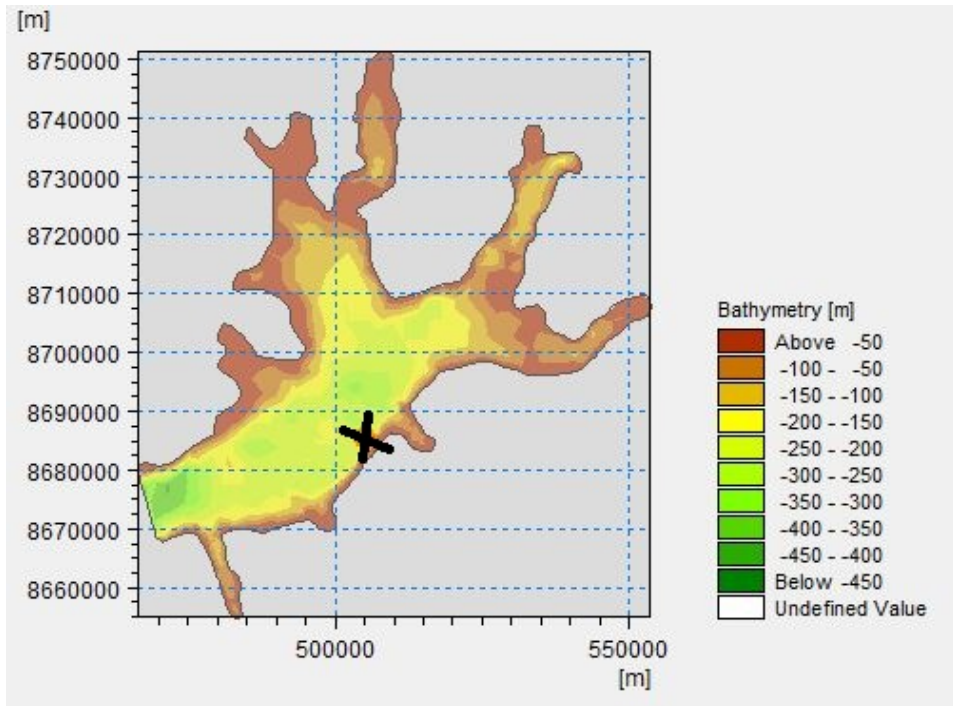


Figure 6.1: Mesh over Bjørndalen with the location the data is extracted from

6.1.1 Run#1, Constant wind data from NMI and tides from C-map

The water elevation from Run#1 can be seen in Figure 6.2. The water elevation is experiencing a small total increase of water level compared to the original water level in Figure 5.11. The currents result from this simulation is shown in Figure 6.3.

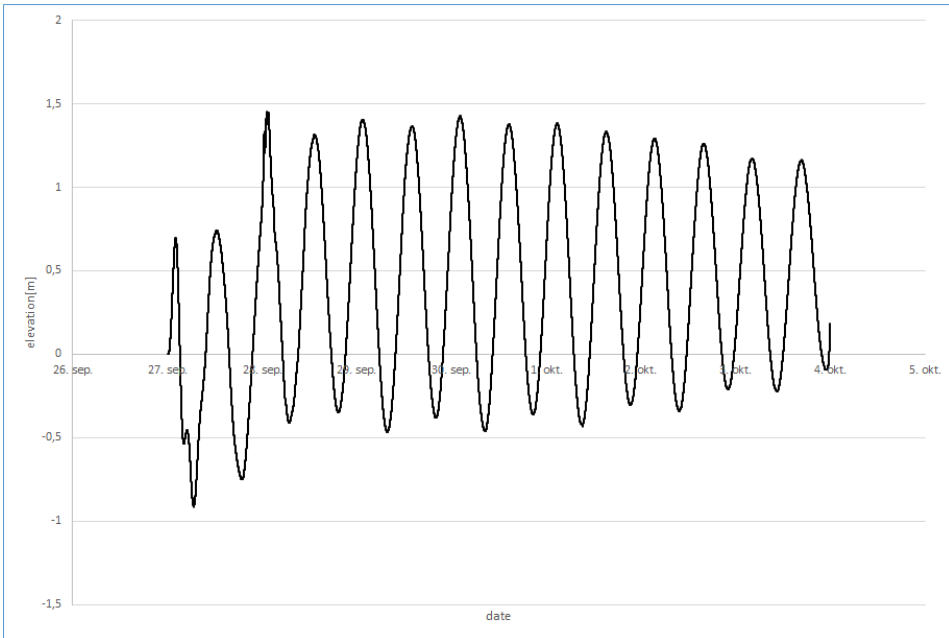


Figure 6.2: Water elevation at Bjørndalen with wind data from NMI, run number one

Figure 6.4 shows the currents at the coastline of Bjørndalen, here the velocities are still large but there are not any unrealistic values at Bjørndalen.

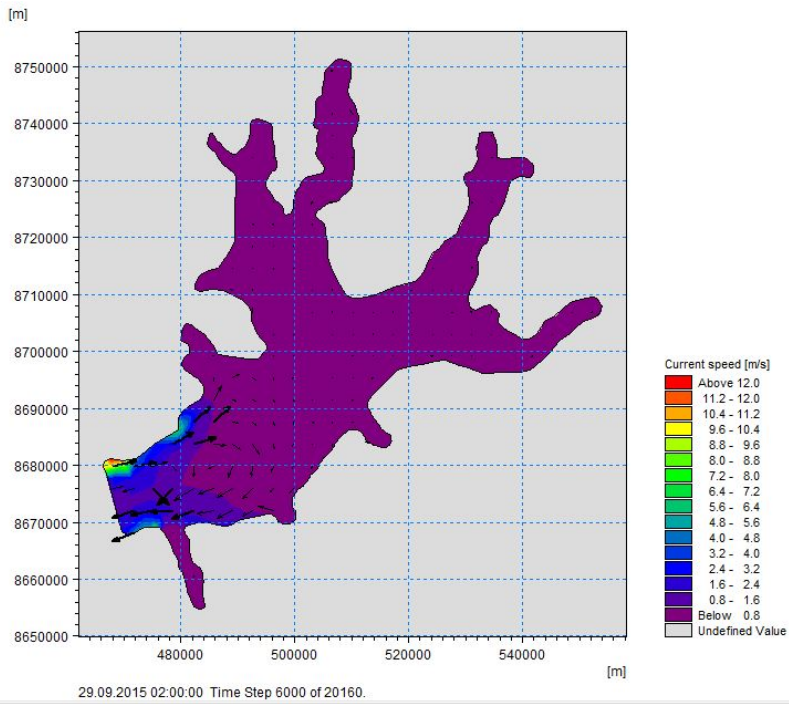


Figure 6.3: Current at Bjørndalen with wind data from NMI

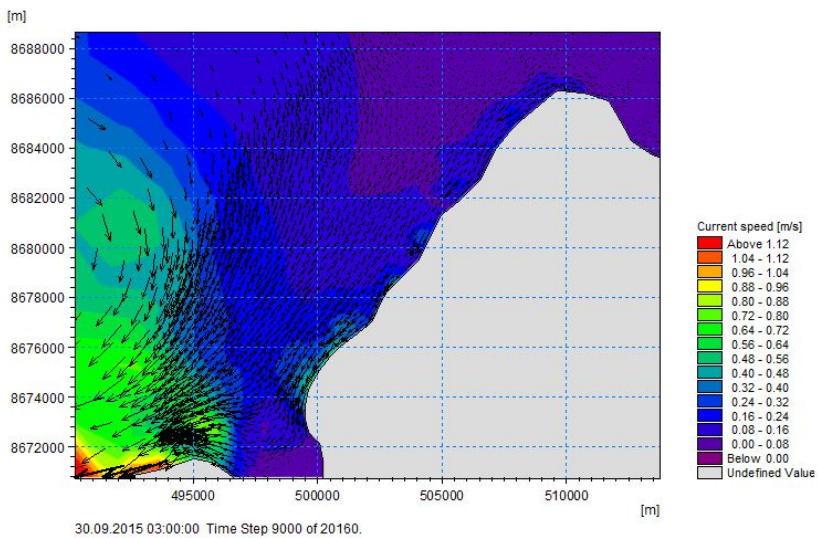


Figure 6.4: Current speed and direction at Bjørndalen caused by wind data from ECMWF and tidal variation

6.1.2 Run# 2: Varying wind data from ECMWF and tides from C-map

The result of water elevation is shown in 6.5. Currents are shown in figure 6.6. The currents exceeds 6m/s at some points close to the entrance, in the rest of the figure the currents are below 2m/s.

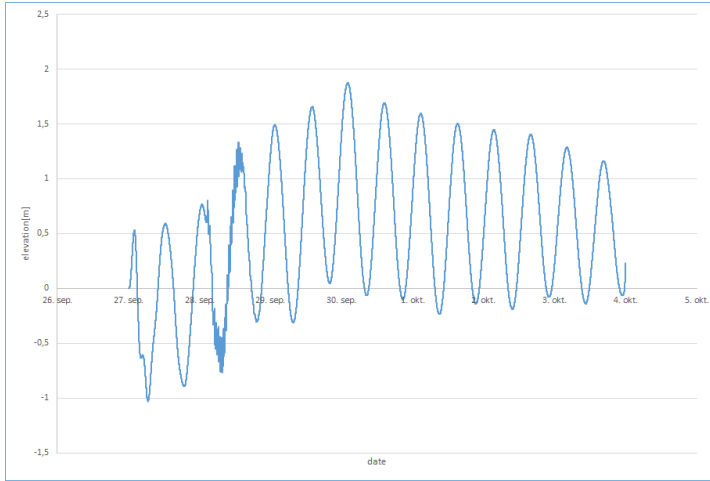


Figure 6.5: Water elevation at Bjørndalen with wind from ECMWF, run number two

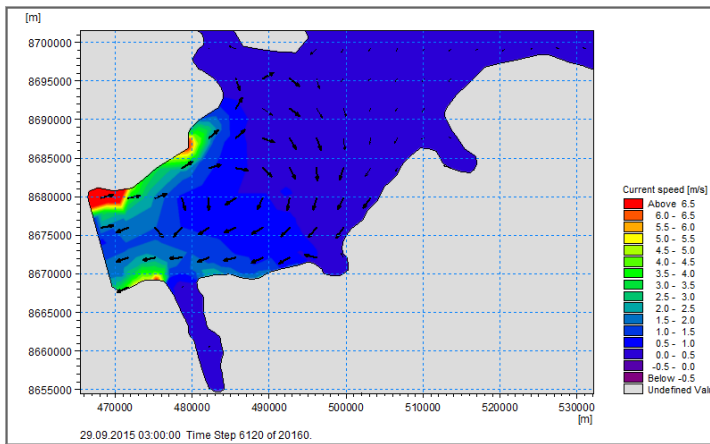


Figure 6.6: Current velocity and current direction at Isfjorden using data from ECMWF

6.1.3 Run#3, Constant Wind Data From NMI, No Tides

The resulting surface elevation from this run is shown in Figure 6.7. Here it becomes a large increase in water elevation close to the time of the storm witch seems presentable and can represent the storm surge caused by the onshore blowing wind at the area. There was reported a large storm surge during the storm(Barstein (2015)). The current because of the wind is shown in figure 6.8.

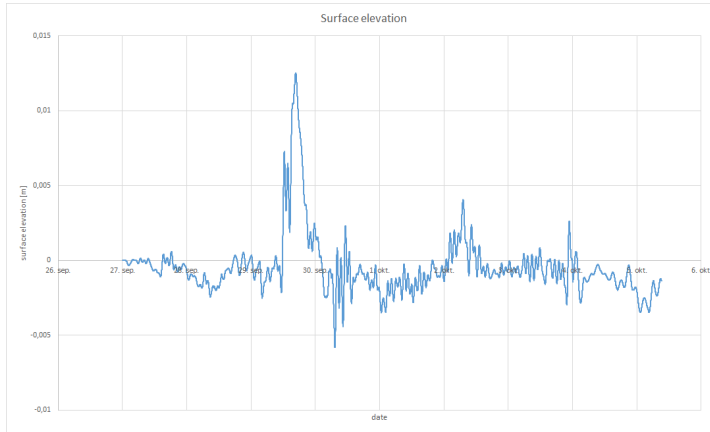


Figure 6.7: Water elevation at Bjørndalen with wind input from NMI and tides are neglected

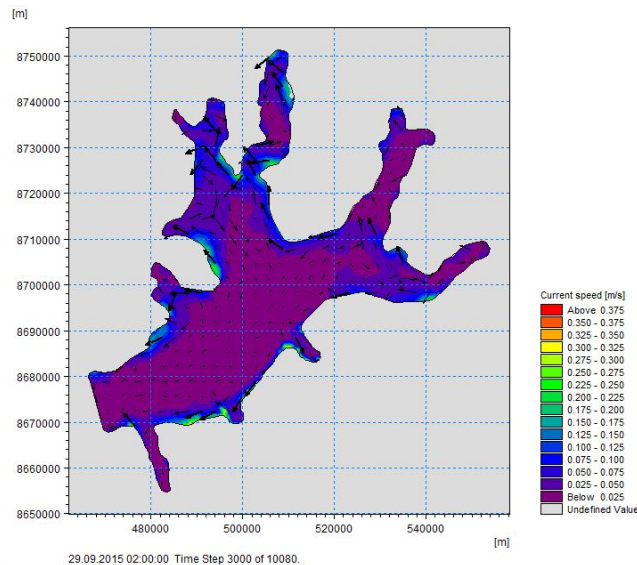


Figure 6.8: Currents in Isfjorden with wind input from NMI and tides are neglected

6.1.4 Run#4: Varying Wind Data From ECMWF, No Tides

Resulting water elevation is shown in Figure 6.9. In this case the water elevation is decreasing during the storm before it is rapidly increasing after the storm. Using this wind field therefore give a decrease in water level during the time of the storm. The current situation because of the wind from ECMWF is given in Figure 6.10

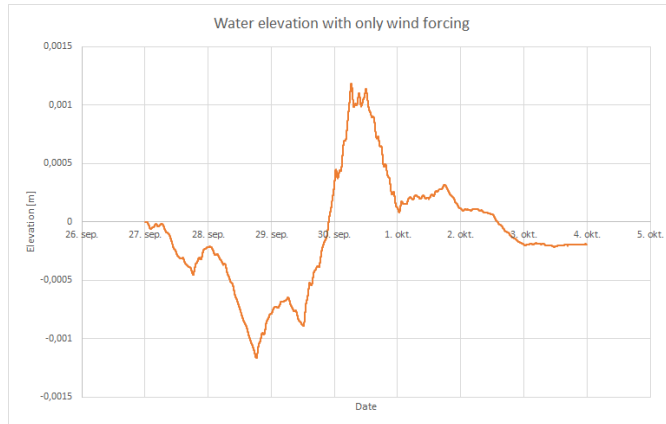


Figure 6.9: Water elevation at Bjørndalen with wind input from ECMWF and tides are neglected

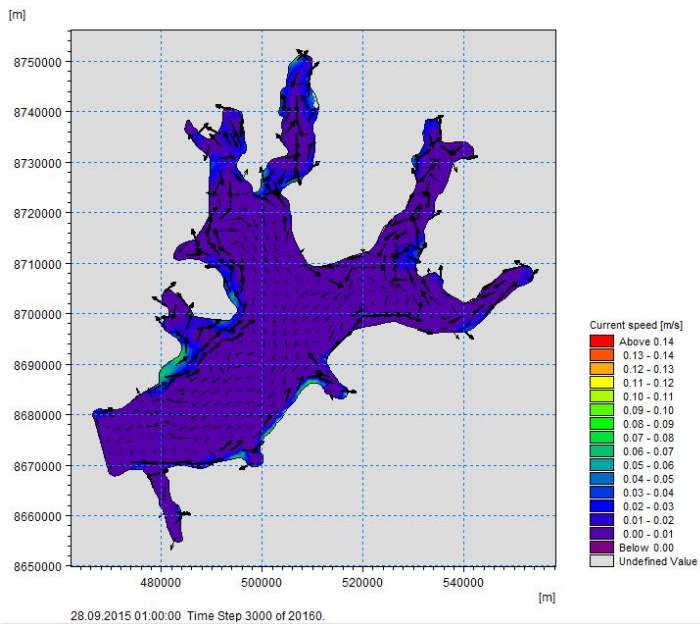


Figure 6.10: Current speed in Isfjorden with wind input from ECMWF and tides are neglected

6.1.5 Discussion

The four runs done with MIKE21 Flow HD shows the effect on surface elevation and currents due to the presence of wind and tides. The tides are mainly depending on the initial tides, but they are varying some because of the wind and pressure induced water elevation.

Currents

The currents is shown in Figures 6.3, 6.6, 6.8 and 6.10. The currents as a result from run#1, has some unrealistic high values at some points in Isfjorden. At the entrance of the fjord close to the boundary the the magnitude of the current are up to 12m/s. In the rest of Isfjorden the currents are large but not unrealistically large, they are under 2 m/s. The currents caused by Run#2 shown in Figure 6.6 have some better values, but still the currents at the entrance of the fjord are unrealistically high. The reason for the high currents can be the numerical modeling fails due to sharp edges at the entrance, not enough to the soft start, the most probable cause is to sharp edges since the currents in the rest of the domain is ok. Sharp edges in the mesh are creating instability in the numerical modeling and can cause large errors that are not physically possible.

The currents for Run#1 are higher than the currents for Run#2. The difference between these two runs comes from the wind conditions. Here a reason for the higher currents for Run#1 can be that the wind is constant over the entire domain. This makes the force from the wind is intensified and wind induced currents occur. Wind from ECMWF will not be able to induce currents in the same direction with the same magnitude as NMI is able to. Another reason for the difference in current values may be that the wind speed are higher for NMI than ECMWF. Zygumt Kowalik (2015) studied the tidal currents in the western Svalbard fjord (Zygumt Kowalik (2015)), in this study the the currents was much lower than the currents that can be seen in the modeling in this thesis. In the studies of the fjord next to Svalbard it is stated that the highest currents is reaching 2 to 3 m/s and this is way below the results found in this modeling (Zygumt Kowalik (2015)).

The currents for Run#3 and Run#4 is more realistic and the values of the currents is shown in Figures 6.8 and 6.10. The highest currents are caused by the wind from NMI, the reason behind this is that the NMI wind is constant while ECMWF is varying over the domain. The currents in these figures are only depending on the wind induced currents and these type of currents are lower than the tidal currents. The same is representative for these four modeling, the tides are the most important cause for the currents in Isfjorden. This indicated that the tides in combinatin with a sharp mesh are causing the instability of the modeling.

Water elevation

The water elevation for Run#1 and 'Run#2 depends on the initial water elevation but there are a small change in the water elevation at Bjørndalen due to the wind. The results in

Figure 6.2 shows a small difference from the initial tidal conditions that was given at the entrance of Isfjorden. Bjørndalen is experiencing an increase of water level on approximately 0.5m in comparison with the initial conditions, this is in the correct range of a storm surge. The water elevation from run number two is given in Figure 6.5, in this figure it is shown that the water elevation is increasing from maximum water elevation on 0.5m to 1.8m before the storm occurs. This is an increase of 1.3m at the time of the storm and this increase might be a bit high due to only wind and tidal variation. This 1.3m comes in addition to the 1.8m difference in low and high tide. After the storm the water elevation is decreasing again, this behavior is what is expected. This can represent the storm surge during the storm, where the peak is indicating at the time of the storm. The water elevation for run number two looks more realistic since it is increasing because of the storm and then decreasing after the storm. While the water elevation because of run number one is increasing in the beginning and stays at the increased level.

The water elevation without tidal variation is investigated to see the importance of the wind and pressure. The two results showing water elevation is shown in Figures 6.7 and 6.9. The magnitude of surface elevation is 0.013m for run number three. This maximum value is at the time of the storm. A water elevation of 0.013m is not a lot and will almost not be noticed in the hydrodynamical forces acting on the shoreline. The maximum value for run number four is 0.0012m. This water elevation is so small that it will not be noticeable. Something strange with the values for run number four is that the surface elevation is decreasing before the storm. This is not expected. From these two runs, number three and number four it can be said that the wind both from NMI and ECMWF does not have any impact on the total surface elevation in the at Bjørndalen.

Where the surface elevation in run number one and run number two comes from is difficult to say when the surface elevation for simulation without tides are neglectable but with tides it is increasing 0.5m for run number one and 1.3m for run number two. Since the wind does not have an impact on the surface elevation the results for run number one and run number three is not what was expected. It would have been expected that the two results would have been almost the same. This should have been investigated more to get more confidence in the results or to know the cause of this behavior.

The results from run number two will be used further in the investigation of the conditions at Bjørndalen. The results from using the wind data from ECMWF is not so different from wind data from NMI and it is possible to see that they behave in the way when modeling with MIKE21 Flow HD, this gives confidence in using the ECMWF in MIKE21 SW and it will give reliable answers.

6.2 MIKE21 Spectral Wave Module Result

6.2.1 Run#1: Offshore Waves From NMI , Varying Wind From ECMWF, Water Elevation and Currents From MIKE21 Flow HD

Figure 6.11 shows the significant and maximum wave height at a location close to the coastline of Bjørndalen. At the time of the storm the wave height at Bjørndalen is at the lowest but starts to increase and reaches its maximum mid day 30th of September. Wind at Bjørndalen is shown in Figure 6.12 and the wind is increasing at the same wave the wave height is increasing. From this observation it is possible to see that the waves significant wave height and maximum wave height depends on the wind at the location. The wind is at the wrong date and this may have something to do with the input wave and not the modeling. Figure 6.12 shows the wind profile at Bjørndalen, the wind is the average over the sampling time of 11 min and 15 sec and this wind is modelled from the data given wind input file from ECMWF.

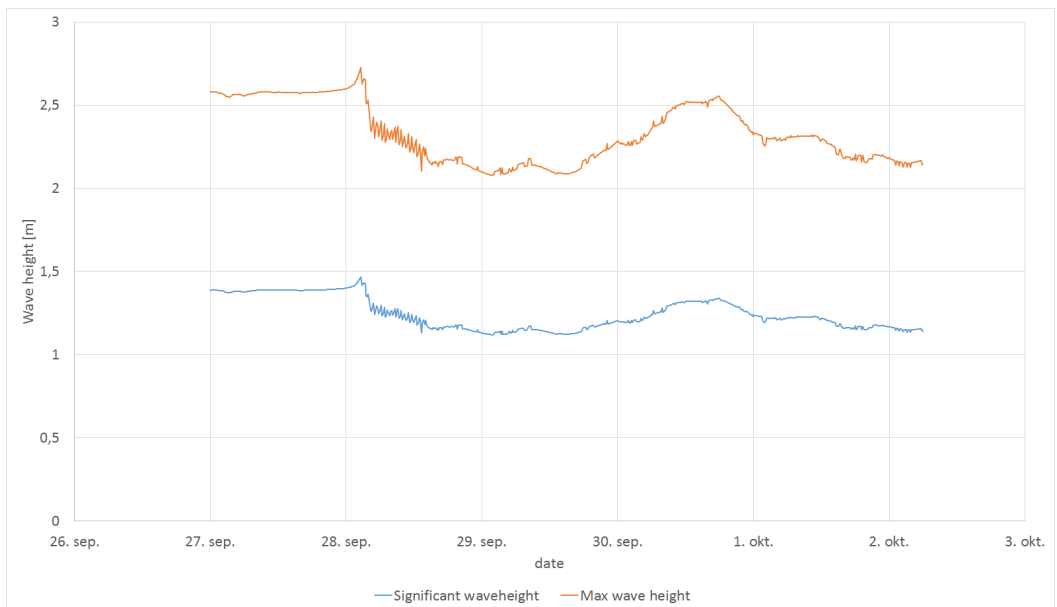


Figure 6.11: Significant (H_s) and maximum wave height (H_{max}) at Bjørndalen

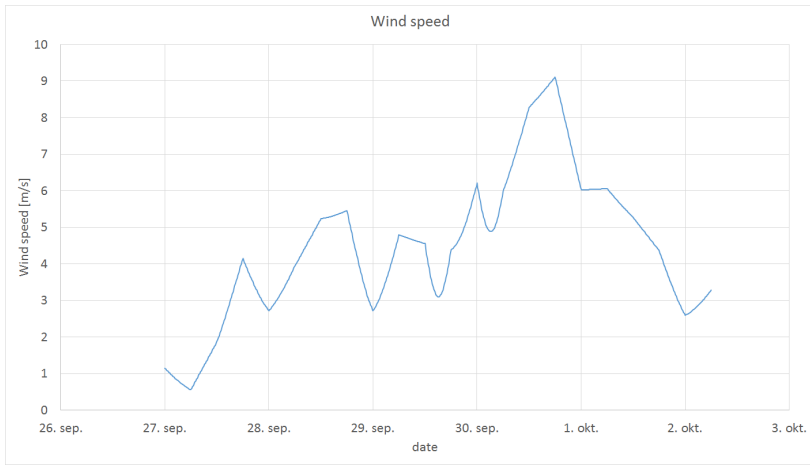


Figure 6.12: Wind velocity at Bjørndalen

Figure 6.13 and 6.14 shows how the waves are changing direction and interacting with the shoreline of Bjørndalen, these figures gives a representation of how the waves are expected to arrive Bjørndalen. The direction of the waves has changed due to refraction. The maximum wave height (H_{max}) found at the area is 3.1m, this is found a distance offshore and the maximum wave height close to shore is 2.6m. The significant wave height (H_s) at the area will vary between 1.6 a distance offshore to 0.9 close to shore.

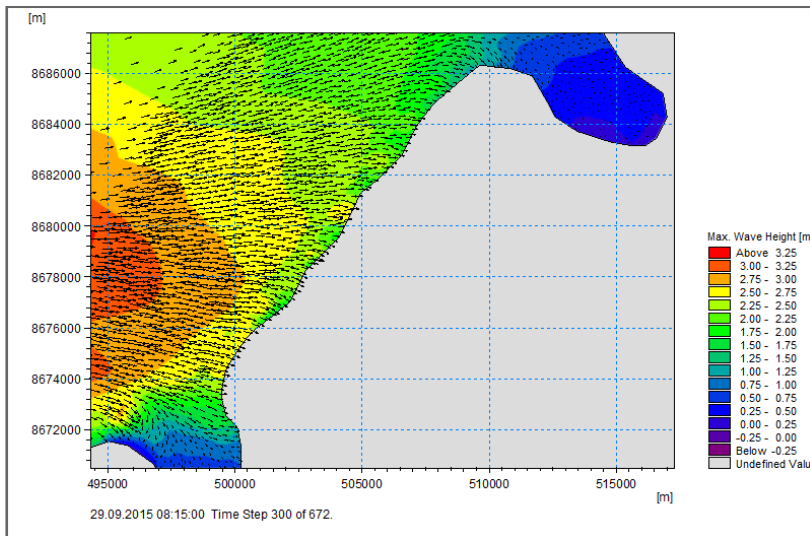


Figure 6.13: Maximum wave height at Bjørndalen

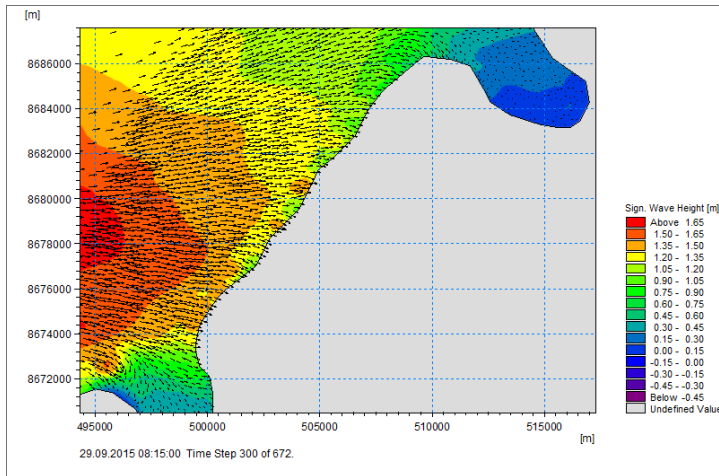


Figure 6.14: Significant wave height at Bjørndalen

The wave period at Bjørndalen is shown in Figure 6.15 where the peak period (T_p) and wave period (T_{01}) is shown. The period T_{01} is 11s for the time of the storm and T_p is 13s at the time of the storm. The wave period is the same as the initial wave period before the storm and is decreasing during the storm. The decreasing wave period is not expected.

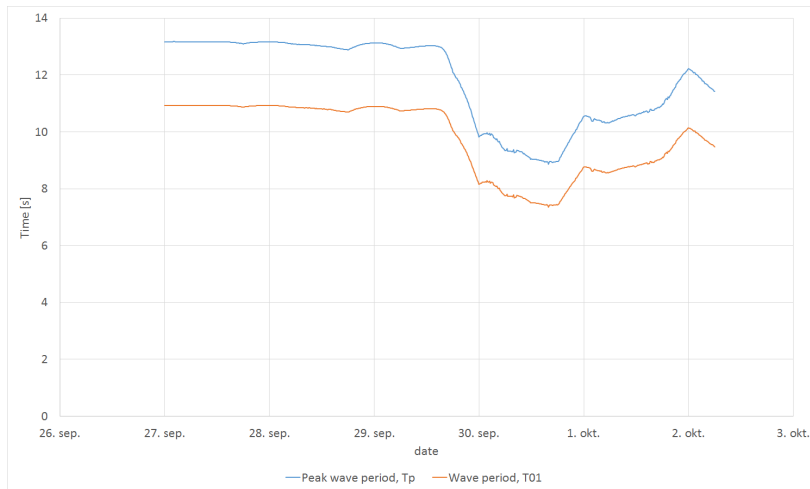


Figure 6.15: Wave period at Bjørndalen

The wave direction are given in Figure 6.16, this figure shows that the direction of the waves has changes from the entrance of Isfjorden to the location where the measurements are taken. The direction the waves are approaching Bjørndalen is between 245 and 275 degrees. The largest waves from an offshore location is arriving Isfjorden from approximately 225 to 250 degrees, shown in Figure 5.11. This indicates that the waves has changed direction due to the topography of Isfjorden, due to the decreasing water depth in Isfjorden this is the expected behavior.

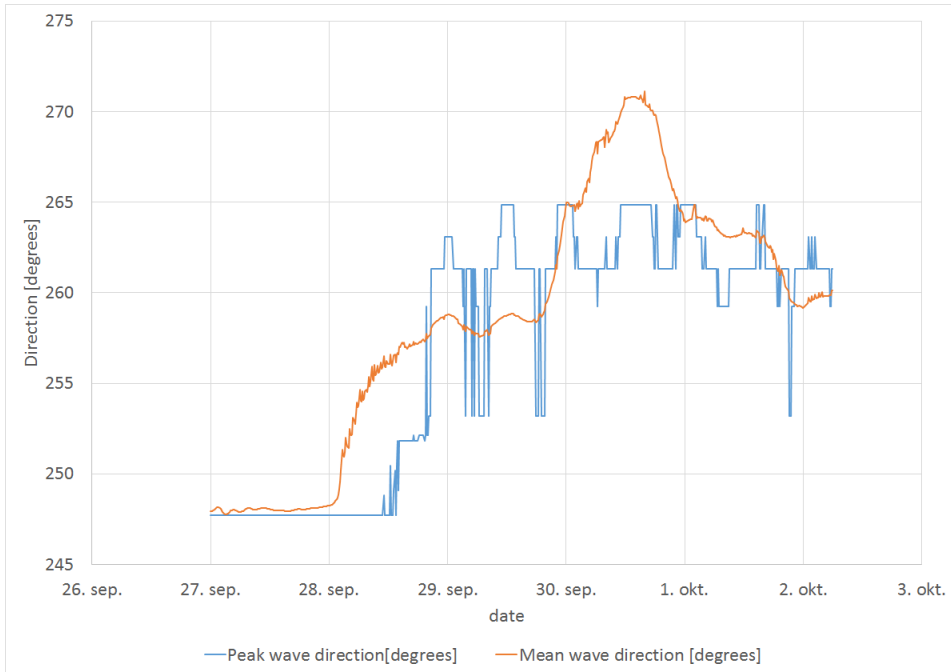


Figure 6.16: Wave direction at Bjørndalen

The radiation stresses is shown in Figure 6.17. The highest radiation stress is approximately $0.45m^3/s^2$ and this is also at its largest after the storm and this is expected since the wind in the modeling is largest after the storm. These values seems to be in the right range of what is expected.

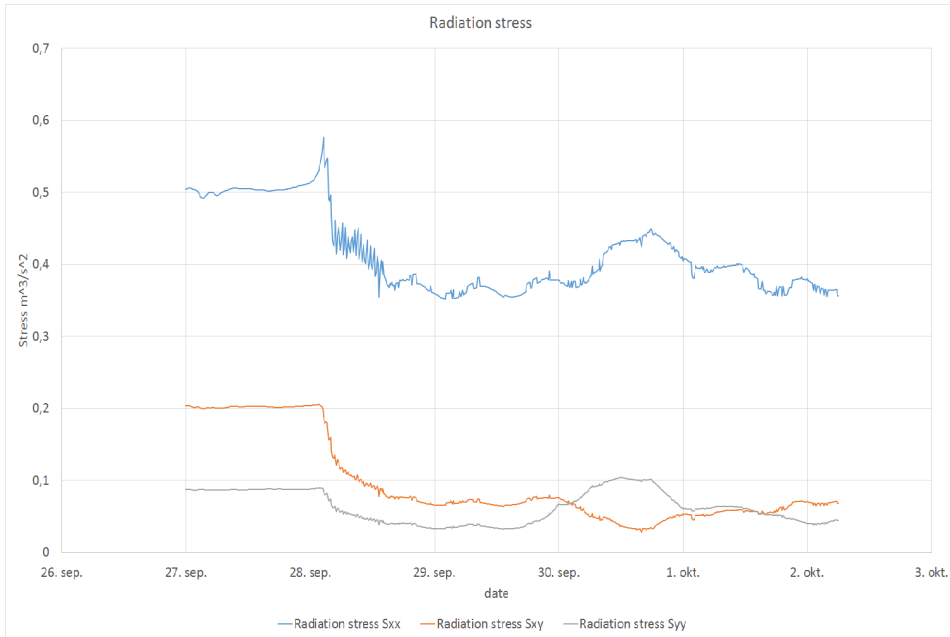


Figure 6.17: Radiation stresses at Bjørndalen

6.2.2 Run#2: Varying Wind from ECMWF, Water Elevation and Currents From MIKE21 Flow HD

The waves calculated by this model is sea and is shown in Figure 6.18. Representing the significant wave height and maximum wave height. The maximum wave height caused by wind inside of Isfjorden is 1.5m. The significant wave height is 0.7 at its maximum, but it is varying between 0.1 m and 0.7m for the time of the storm. These maximum values are occurring when the wind is at its maximum.

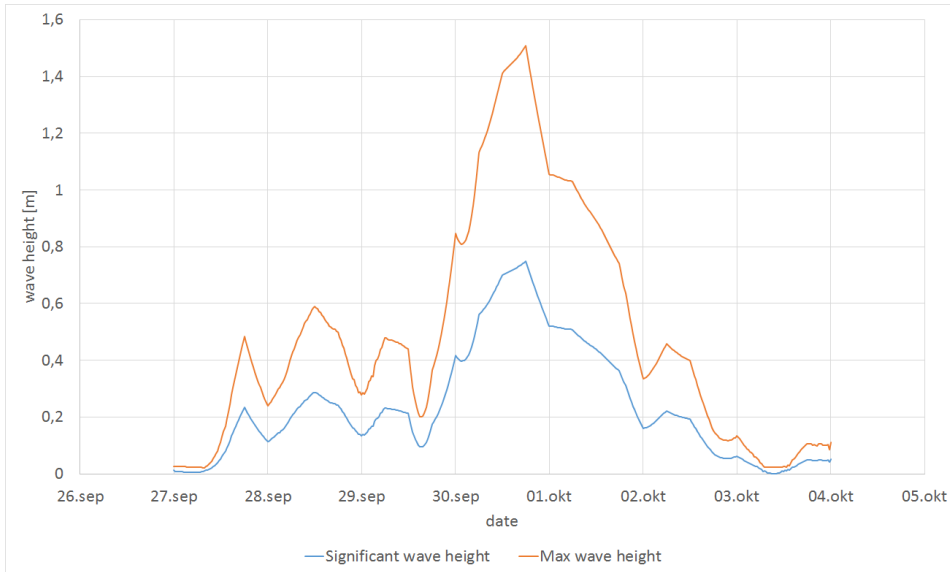


Figure 6.18: Wave height at Bjørndalen when swell are neglected

The wave period for the case when swell are neglected is illustrated in Figure 6.19. The wave period is varying between 0.5s and 4s, this is a good representation of sea waves as they are characterised as small period waves with small wave height.

The radiation stresses for only wind waves is shown in figure 6.20 and the maximum value is $0.1 \text{ m}^3/\text{s}^2$, while with waves included the maximum radiation stress was $0.45 \text{ m}^3/\text{s}^2$. The radiation stresses due to the sea is small and can be neglected, compared to radiation stresses when swell is included.

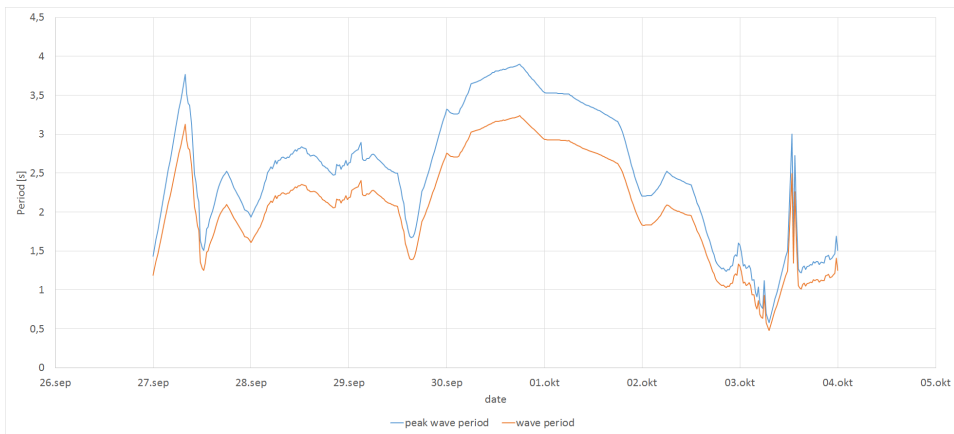


Figure 6.19: Wave period at Bjørndalen, when swell are neglected

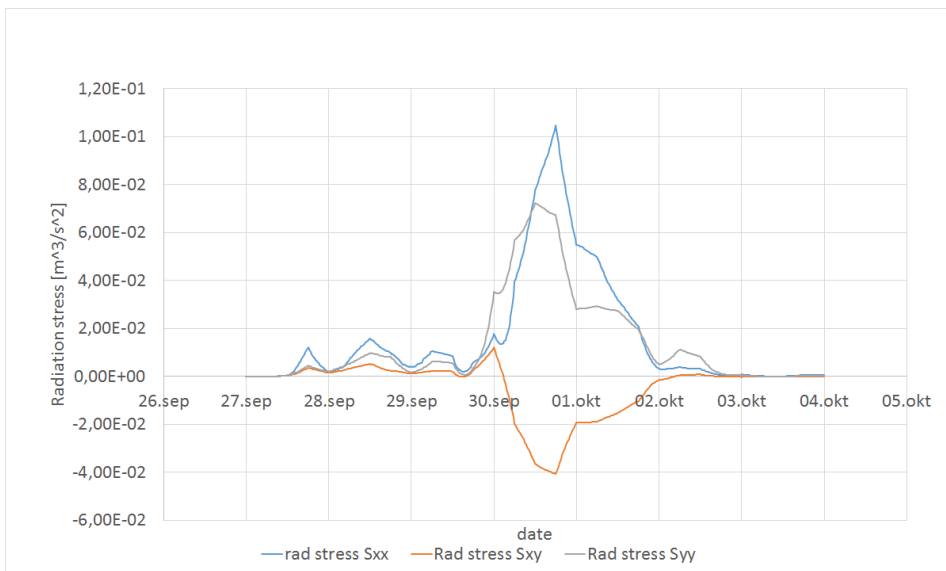


Figure 6.20: Radiation stress at Bjørndalen when swell are neglected

Figure 6.21 shows the currents in Bjørndalen when swell are neglected. The graph has some unexpected behavior in the beginning of the simulation before it smooths out. Figure 6.21 shows that the currents are varying between 0.01 m/s and 0.1 m/s.

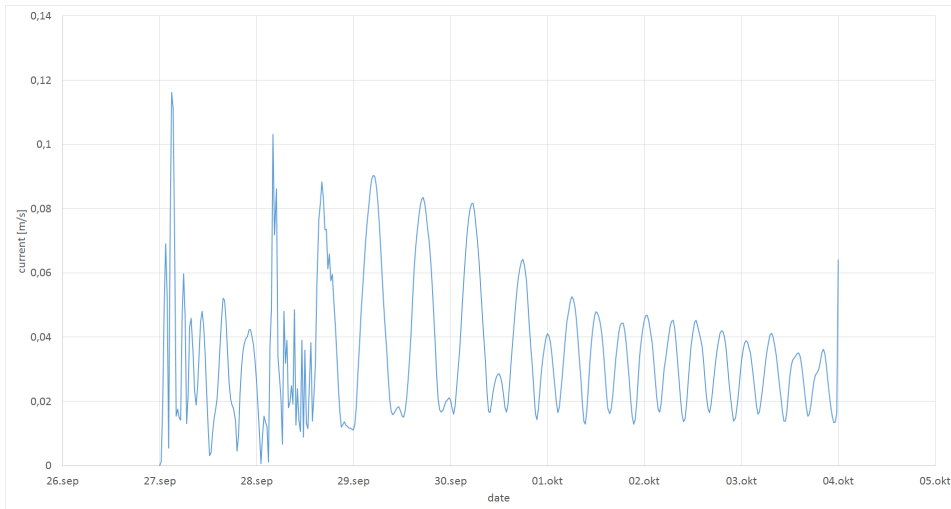


Figure 6.21: Current at Bjørndalen when swell are neglected

6.2.3 Run#3: Offshore Waves From NMI, Water Elevation and Currents From MIKE21 Flow HD

The wave height calculated in run number three is shown in Figure 6.22. Here the wave height is constant during the entire simulation period. This is due to the way the waves are included in the model. The waves are included with wave parameters at the boundary and are not varying over time. The maximum wave height is 2.1m and the significant wave height is 1.1m.

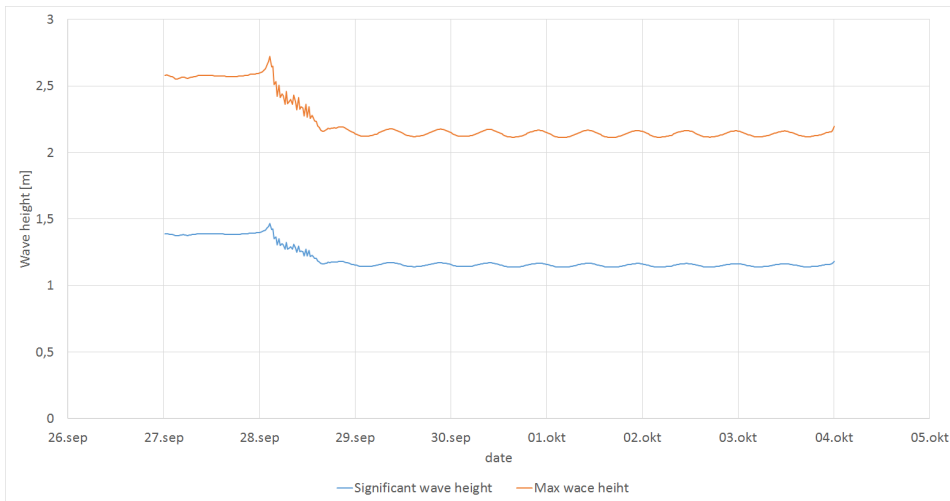


Figure 6.22: Wave height at Bjørndalen when wind is neglected

Figure 6.23 shows the current velocity at Bjørndalen when wind is neglected from the modeling. The grey line is representing the total velocity, orange and blue represents the velocities in x and y direction. The velocity at Bjørndalen is varying between 0.01 m/s and 0.1 m/s.

Radiation stresses are shown in Figure 6.24. The maximum value is $0.38 \text{ m}^3/\text{s}^2$ and it is constant during the modeling time. Some adjustments from the program occurs in the beginning.

The wave period is shown in Figure 6.25. The period is not varying over time, this is due to the way the offshore waves are included in the model. The peak wave period is 13s and the wave period T_{01} is 11s.

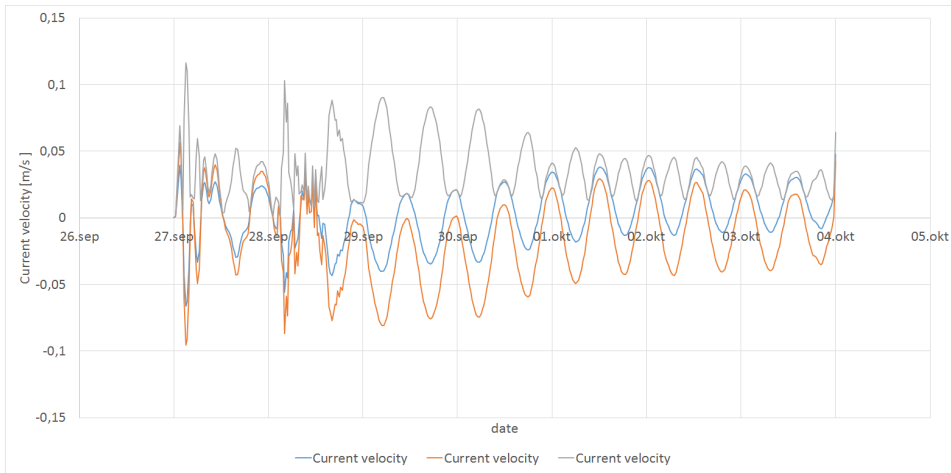


Figure 6.23: Current velocity at Bjørndalen when wind is neglected

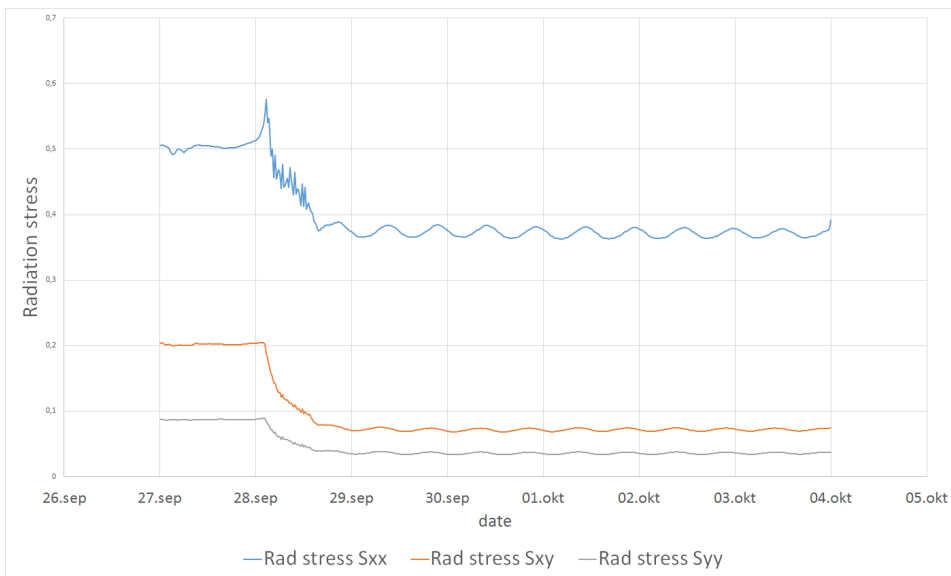


Figure 6.24: Radiation stresses at Bjørndalen when wind is neglected

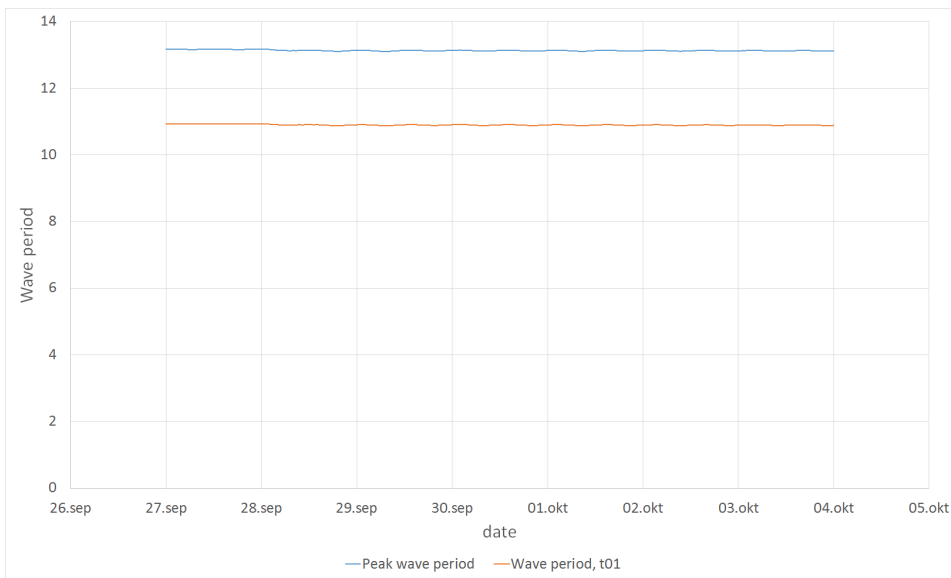


Figure 6.25: Wave period at Bjørndalen when wind is neglected

6.3 Discussion

Wave Period

The wave period for the most energetic waves are mostly depending on the offshore waves. However, it is possible to see some changes due to the presence of sea.

Wave Height

Swell are entering the fjord and is the main contribution to the significant wave height propagating towards Bjørndalen. The largest waves comes from an offshore location, without the swell the wave in Isfjorden would be small. Sea waves contribute to a small increase in the wave height, both significant and maximum wave height. When the swell and sea are combined it generates larger waves. The waves coming in as swell are calculated to be constant over the period of the simulation. If the waves were included as a time series the representation of the situation would be more realistic. If the waves were varied over time the significant wave height should have been higher during the storm. The wave conditions are input parameters calculated using the average over the modeling period. The small wave heights before and after the storm will decrease the significant wave height. The maximum wave height modelled is therefore smaller than the wave height expected by the data collected and modelled from NMI. In this case the wave conditions are underestimated. When investigating the wave height of the swell modelled by the NMI of 4.25m at the time of the storm, the wave height during the storm should have been higher than the modelled wave height. The wave height modelled by NMI is shown in Figure 5.10.

The total wave period is dependent on the swell and some small changes accrue due to the wave periods from the sea. This is shown in Figure 6.25 where the period is constant during the entire modeling period and it is varying over the modeling time in Figure 6.15 showing the wave period when swell and sea are included. The wave period is mainly based on the swell but will decrease some because of the period of the swell.

Radiation Stress

The radiation stress is a result of surface gravity waves and from the graphs in Figures 6.17 and 6.20 the radiation stresses for swell and sea waves combined are much higher than for only sea waves. The main contribution of radiation stresses comes from swell. There will then be an angle between the waves and the shoreline and a cross shore current will arise due to the radiation stresses. This current will be in the opposite direction of the natural currents caused by the tides. The currents in this area are therefore expected to decrease but it is increasing at the coast of Bjørndalen.

Currents

The currents experience changes from the initial condition due to the presence of waves and the radiation stresses caused by the waves. The changes are shown in Figure 6.26, here the grey line represents the currents before waves was introduces and the orange is the currents when waves are included. The expected result would have been an decrease in the currents along Bjørndalen. This is not the case, the currents are increasing with 0.01m/s. It is expected because the waves will push the currents to propagate in an different direction than the currents.

The results for wave height, wave period, radiation stresses and currents show irregularities at the beginning of the simulation. This indicates that the model needs time to adjust before it smooths out and shows more representable data. Probably the analysis should have been modelled from an earlier date so the model would have time to adjust in good time before the time of the storm.

6.3.1 Discussion

Figure 6.26 shows the comparison of the currents at Svalbard.

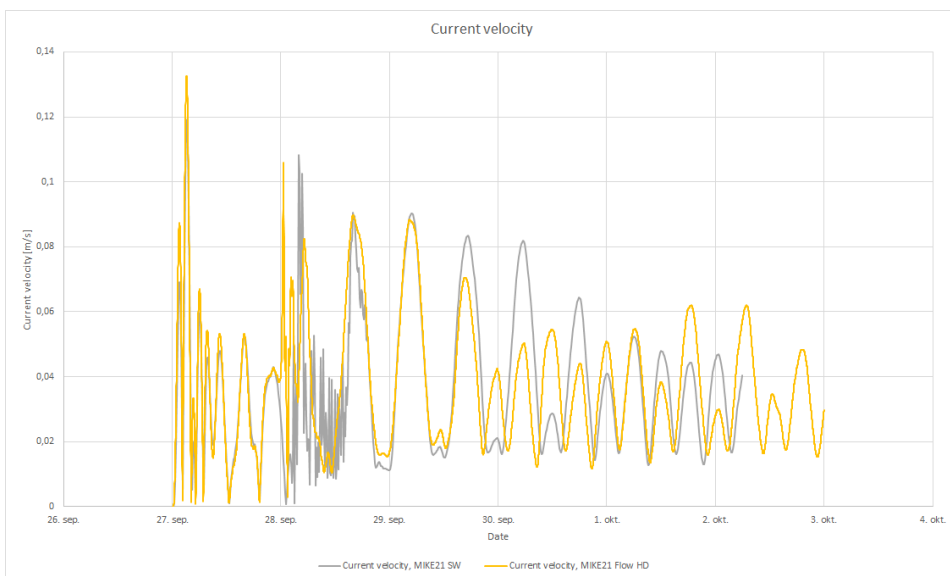


Figure 6.26: Current at Bjørndalen

6.4 Sediment Transport

Since there was no time to investigate the sediment transport and coastal erosion at the site, this is recommended for future work. This is important to investigate to be able to protect the areas at risk and develop cheap and reliable methods to prevent and protect the coastal area. In this modeling the MIKE21 ST can be used to see if it gives some answers that fit the natural processes.

Conclusion and Recommendation

7.1 Summary

The results from the various runs gives an understanding on how the different input factor are and how they contribute in changing the environment in the fjord. There are some results that does not behave as expected. This behavior can be transferred back to the input parameters or the setup of the model. MIKE21 gives a good representation of the hydrodynamic conditions in Isfjorden.

The currents at Bjørndalen are high due to the tidal currents, this currents are not affected by wave induced currents from radiation stresses. The studies from Zygmunt Kowalik (2015) confirms that it is normal with high currents in The fjords at Svalbard.

The large unrealistically values at the entrance of Isfjorden is probably caused by instability in the numerical modelling. Sharp edges in the mesh can be the reason for this instability.

The currents caused by swell and sea is not giving as much change to the currents as expected. This can be because of the large currents caused by tidal variations. The rest of the results gives a better representations of the situation in Bjørndalen. The waves will give large forces on the coastal zone. The waves are probably underestimated due to the way waves are included in the model. The small waves are also causing smaller values of radiation stresses.

The offshore waves are the main contribution for large waves interacting with the shoreline. It can therefor be concluded that the largest forces occurring from the offshore wind waves. These wind waves may have been modelled to be smaller than they really are. A better to represent the offshore waves are desirable.

The water elevation on 1.8m is high, but this high storm surge makes the waves reach high up on the shoreline and can be a reason for large erosion even with waves that does not have an extreme value.

7.2 Recommendation For Further Work

The erosion of coastal Arctic areas are an increasing problem, so to investigate the results of a storm in the Arctic region is recommended. This is a area that needs more investigation and good tools to be able to predict erosion of the coastline. The Arctic has problems that are not an issue in temperate areas as frozen soil and presence of sea ice.

Bibliography

- Ashbindu Singh, Sumith Pathirana, H. S., 2006. Assessing coastal vulnerability : developing a global index for measuring risk. Nairobi : United Nations Environment Programme, 2006.
- B. M. Jones, C. D. Arp, M. T. J. K. M. H. J. A. S., Flint, P. L., 2009. Increase in the rate and uniformity of coastline erosion in arctic alaska. *GEOPHYSICAL RESEARCH LETTERS* 9, 5.
- Barstein, G., October 2015. Slår erosjonsalarm: Hytter og veien til bjørndalen kan rase på havet når som helst.
URL <http://svalbardposten.no/nyheter/natur-og-miljo/hytter-og-veien-til-bjorndalen-kan-rase-pa-havet-nar-som-helst/19.6410>
- BBC, May 2016. Coastlines of erosion and deposition.
URL <http://www.bbc.co.uk/education/guides/z3ndmp3/revision/3>
- Bretschneider, C. L., 1952. The generation and decay of wind waves in deep water. *EOS, Earth and space science news*, 9.
- DHI, June 2015. Mike 21 2d modelling of coast and sea.
URL <http://www.mikepoweredbydhi.com/products/mike-21>
- Donald L. Forbes, Volker Rachold, H. K. H. L., 2010. State of the arctic coast 2010 scientific review and outlook. International Arctic Science Committee, Land-Ocean Interactions in the Coastal Zone, Arctic Monitoring and Assessment Programme, International Permafrost Association, 178.
- et Al, L. R., 2009. Landforms and sediments, bjørndalen-vestpynten, svalbard. *SCIENCE*, 2.
- F. Gunther, P. P. Overduin, A. V. S. G. G., Grigoriev, M. N., 2013. Short- and long-term thermo-erosion of ice-rich permafrost coasts in the laptev sea region. *Biogeosciences*, 22.

-
- forecast database(ECMWF), E. M.-R. W., January 2015. Home page of ecmwf.
URL <http://www.ecmwf.int/>
- Fredsøe, J., Deigaard, R., 1992. Mechanics of coastal sediment transport. World Scientific.
- Galvin, C. J., 2016. Breaker type classification on three laboratory beaches. U.S. Army Coastal Engineering Research Center, Washington, 9.
- group, D., 2016a. Mike 21 flow model fm, hydrodynamic module. DHI manual HD, 142.
- group, D., 2016b. Mike 21 spectral waves fm, spectral wave module. DHI manual SW, 122.
- group, D., 2016c. Mike 21 st, non-cohesive sediment transport module. DHI manual ST, 122.
- Gugan, E. B. M., Christiansen, H. H., 2016a. Seasonal arctic coastal bluff dynamics in adventfjorden, svalbard. PERMAFROST AND PERIGLACIAL PROCESSES, 14.
- Gugan, E. B. M., Christiansen, H. H., 2016b. Seasonal arctic coastal bluff dynamics in adventfjorden, svalbard. John Wiley Sons, Ltd, 14.
- hurricane center, N., may 2016. Storm surge overview.
URL <http://www.nhc.noaa.gov/surge/>
- Jeppesen, January 2015. Mike c-map, model bathymetries made fast and easy.
URL <https://www.mikepoweredbydhi.com/products/mike-c-map>
- Kamphuis, J. W., 2010. Introduction to coastal engineering and management. World Scientific.
- Krogstad, H. E., Arntsen, o. A., 2003. Linear Wave description and Theory. Norwegian University of Science and Technology.
- LONGUET-HIGGINS, M. S., STEWART, R. W., 1964. Radiation stresses in water waves; a physical discussion, with applications. Pergamon Press Ltd., 34.
- Martin Beniston, David B. Stephenson, O. B. C. C. A. T. F. C. F. S. G. K. H. T. H. K. J. B. K. J. P. R. S. T. S., Woth, K., 2007. Future extreme events in european climate: an exploration of regional climate model projections. Springer Science + Business Media, 25.
- NASA, Febuary 2016a. Arctic sea ice minimum.
URL <http://climate.nasa.gov/vital-signs/arctic-sea-ice/>
- NASA, Febuary 2016b. Climate change: How do we know?
URL <http://climate.nasa.gov/evidence/>
- Pawe Rowinski, Marek Banaszkiwicz, J. P. M. L. M. S., 2014. Fluvial Hydrodynamics, Hydrodynamic and Sediment Transport Phenomena. Springer.

-
- Pgengsheng Wei, James Brethour, M. G., Burnham, J., 2014. Sedimentation scour model. Flow Science Report 03-14 17, 29.
- Rafael E. Vasquez¹, Carl D. Crane, I., Correa, J. C., 2014. Analysis of a planar tensegrity mechanism for ocean wave energy harvesting. JOURNAL OF MECHANISMS AND ROBOTICS 6 (3), 12.
- Roelvink, D., Reniers, A., 2012. A guide to modeling Coastal Morphology. World Scientific.
- S. A. Hsu, E. A. M., Gilhousen, D. B., 1994. Determining power-law wind profile exponent under near-natural stability conditions at sea. Journal of Applied Meteorology and Climatology, 9.
- Sorensen, R. M., 1997. Basic coastal engineering. Springer science + Business media B.V.
- Swamee, P. K., Ojha, C. S. P., 1991. Drag coefficient and fall velocity of nonspherical particles. J. Hydraul. Eng 17, 660–667.
- van Rijn, L. C., 1984. Sediment transport, part i: Bed load transport. J. Hydraul. Eng., 26.
- Volker Rachold, Feliks E. Are, D. E. A. G. C. S. M. S., 2004. Arctic coastal dynamics (acd): an introduction. Geo-Mar Lett, 6.
- Wiki, S. R., may 2016. Sediment transport processes.
URL <https://riverrestoration.wikispaces.com/Sediment+transport+processes>
- Zygmunt Kowalik, Aleksey Marchenko, D. B. N. M., 2015. Tidal currents in the western svalbard fjords. Oceanologia, 10.
